Relating different regularization schemes in Functional Renormalization

Master thesis of
Arthur Vereijken

Supervised by Dr. Frank Saueressig

Theoretical High Energy Physics
Radboud University Nijmegen

March 14, 2019

Abstract

Functional renormalization group methods are powerful tools for studying properties of statistical systems and quantum field theories beyond perturbation theory. A key open question in applying functional renormalization group methods concerns the proper choice of regulator. While the regulator itself is unphysical and should therefore not affect observable quantities, approximate solutions of the functional renormalization group equation may exhibit strong regulator effects. In this thesis we will introduce the functional renormalization group for quantum gravity, after which we will investigate these regulator effects. This leads to a proposal for a relation between renormalization group flows with different regulators, as well as some insights in how terms are generated by the regulator. This proposal is analyzed in a quantum gravity scenario, and we suggest improvements for approximations so that they are more suitable for compensating regulator effects.

Contents

1 Introduction

There are four fundamental interactions in Nature that we currently know of. These are the electromagnetic force, the weak nuclear force, the strong nuclear force, and gravity. Every interaction but gravity is described by the Standard Model of particle physics, which has been extremely successful in predicting experimental observations, such as the anomalous magnetic dipole moment, and the existence of multiple particles, including the W and Z bosons, and famously the Higgs boson. Gravity is described classically by the theory of General Relativity. However when we try to quantize General Relativity in the same way as the other forces in order to incorporate gravity into the Standard Model, we find that this does not work. The reason for this is that General Relativity is non-renormalizable in perturbation theory [3, 4], while the Standard Model is proven to be renormalizable [5]. Renormalization is historically a technique used to deal with infinities in perturbation theory which appear in loop integrals due to self-interaction. The self-interaction changes the coupling constants of the theory, such as the mass and charge of a particle. These constants need to be measured by experiment, and the theory is then expressed in terms of the measured quantities. To this effect one introduces counterterms which cancel the troublesome infinities. As a result, the coupling constants take on the measured value of an experiment *at a certain energy scale*, hence these couplings are no longer constant, but gain a dependence on the energy scale of the system.

The modern viewpoint of renormalization focuses on observing the same physical system at different scales. In this view, the perturbative approach accounts for the fact that the theory does not extend to arbitrarily high energy scales. The unknown high energy behaviour is integrated out by taking experimental values for the couplings. The details of these high energy interactions do not influence the result of the renormalization (which is good, because we do not know these high energy physics). In general, this process will not always work. This is the case if, when increasing the perturbation order, the number of infinities also increases. This has the result that more and more parameters need to be determined by experiment the further one goes in perturbation theory. With increasing energy, the theory gradually loses its predictive power and eventually it would break down. At some point, increasing the perturbation order will decrease the theory's predictive power, because the increased precision will be offset by the new undetermined parameters it introduces. In this case, we speak of an effective quantum field theory: it effectively describes low energy physics and accounts for some quantum effects, but it does not describe fundamental interactions. This is the case for General Relativity, because of its infinite number of counter-terms.

The reasons to search for a fundamental theory of quantum gravity are mostly theoretical in nature. However, from the point of view of experiments or observations, we would also require a theory of quantum gravity which is valid for high energy scales. This is because of the relative strength of gravity in comparison to other fundamental forces: the gravitational force is exceptionally weak. This is obvious when comparing the values of physical constants, and a common way of illustrating this is with small magnets, for example fridge magnets. Their magnetic force is able to equal the attractive force of the entire earth and so they stay stuck to your fridge. The energy scale at which quantum gravity effects are significant is then extremely high; it is around what we call the Planck Scale, which is at approximately 10^{18} GeV. To put this in perspective: state-of-the-art particle accelerators such as the LHC where the Higgs boson was found accelerate particles to energies around 10^4 GeV, and the highest energy cosmic ray particles detected so far have energies of about 10^{11} GeV. Obviously it is not possible to do experiments at this scale in the lab. Observations are possible in some phenomenologically interesting areas, such as the early universe, in particular inflation; and black holes. However, current observational knowledge about these areas still fits a wide variety of models and so only gives limited restrictions on our possibilities.

Given that we cannot make a theory of quantum gravity via the usual route of renormalized perturbation theory, it is common to argue for a theory beyond an ordinary quantum field theory, or adding extra principles, such as further symmetries; extra dimensions, strings; or holography. On the other hand, one can also extend the perturbative methods used in quantum field theory, since it is (formally) defined without perturbation theory. These approaches, such as Causal Dynamical Triangulation (CDT) or Asymptotic Safety, aim to define and compute quantum gravity effects by using the path integral[1]. Instead of abandoning quantum field theory entirely, these approaches generalize perturbative techniques; Asymptotic Safety in particular generalizes the perturbative concepts of renormalization and renormalizability.

The name Asymptotic Safety originates from Weinberg in the late 1970's [6], when he proposed the idea of the existence of a non-perturbatively renormalizable, or asymptotically safe quantum theory of gravity. The Asymptotic Safety approach is based on the generalized notion of renormalization pioneered by Kadanoff and Wilson, in which infinitesimal momentum shells are successively integrated out. The result of this integration is then absorbed in the coupling constants, which flow as a result. The flow of the couplings is governed by a functional renormalization group equation, based on concepts of modern statistical field theory. At the core of this approach is a fixed point of the renormalization group flow. Convergence to this fixed point for increasing energy scale implies a well-defined behaviour for arbitrarily high energies. The theory would then be safe from physically harmful divergences and remain predictive up to the highest energies just like an asymptotically free theory would, except the theory does not converge to the free theory with zero couplings, but to some interacting theory with nonzero couplings. The behaviour in the vicinity of the fixed point is also physically relevant, in particular for critical exponents. Only in the 1990's machinery was developed that allows the study of functional renormalization group methods for the gravitational field [11], kickstarting the field of Asymptotic Safety[2] from then on.

1.1 Asymptotically safe quantum gravity

As stated before, the final goal of Asymptotic Safety and other quantum gravity programs which retain standard quantum field theory or statistical field theory is giving a mathematically precise meaning to, and computing functional integrals, interpreted as sums over all Euclidean spacetime metrics. Schematically:

$$\int D\widehat{g}_{\mu\nu} e^{-S[\widehat{g}_{\mu\nu}]}. \tag{1.1}$$

From this all quantities of physical interest can be derived. $S[\widehat{g}_{\mu\nu}]$ stands for the bare (classical) action, which is invariant under diffeomorphism (a change in spacetime coordinates, effectively stating that the equations it implies hold for any observer), but is otherwise kept arbitrary. In General Relativity this bare action is the Einstein-Hilbert action, but keeping the action general is a key point to Asymptotic Safety: the viewpoint is that the functional integral would only exist for certain actions S and the aim is to identify these actions. The approach to this problem is done in a rather indirect way: the integral is not computed or explicitly constructed, but instead is interpreted as a solution to a certain differential equation, named the functional

[1] Asymptotic Safety uses the path integral in a somewhat indirect way, as we shall discuss further on.

[2] Often, the name "Asymptotic Safety" is used when referring to applications of the funtional renormalization group in order to construct a theory of quantum gravity. In other cases it is called functional renormalization or nonperturbative renormalization. Because the main focus of this thesis is more on general considerations of functional renormalization and not gravity in particular, the title does not contain the words "Asymptotic Safety". However, a quantum gravity scenario *is* where we will apply these considerations.

renormalization group equation, or FRGE. The theory can then be defined through the FRGE and its solutions. In contrast to the functional integral, the FRGE is manifestly well-defined. It is seen as the evolution equation of an infinite dimensional system in which the RG scale plays the role of time. The task of defining functional integrals is then reformulated to finding dynamical systems which extend to arbitrarily high energy scales. This is ensured by the system possessing a fixed point, a point where this evolution stops, which is approached at high energy scales. This gives a well-defined, fully extendable evolution, which tells us how to construct the functional integral.

Just like there are equations of motion for a classical field theory, which are found by requiring the classical action S to be stationary, a quantum field theory has a similar structure. The expectation value $\langle h(x) \rangle$ of some quantum field $h(x)$ is governed by laws described in terms of the effective action Γ. The effective action is a functional similar to the classical action. It can be seen as the quantum mechanical analogue of the classical action, since the dynamical equations for the field expectation values are also found by requiring the effective action to be stationary. Furthermore, it reduces to S in the classical limit, and as such is a generalization of the classical action. Finally, the effective action generates a special kind of expectation value from which all others can be reconstructed, so that finding Γ is often considered equivalent to solving the theory.

Asymptotic Safety then uses the FRGE as its central object. It is the flow equation for a modified definition of the effective action equipped with cutoffs that suppress very long (infrared) and very short distance (ultraviolet) effects. This can also be interpreted in terms of energy or momentum: short distance effects correspond to high energy while long distance modes have low energy. The infrared cutoff is implemented in a specific way, which gives us the Effective Average Action Γ_k, and allows us to derive an evolution equation for Γ_k: the FRGE. The FRGE describes how Γ_k changes with the scale k at which the infrared cutoff sets in. This evolution equation is well-defined even when the ultraviolet cutoff is removed, and is then used as the new starting point of the analysis. In practice, an ansatz will be made for the form of Γ_k. Given this ansatz, the evolution equation is worked out and fixed points are searched for. Existence of fixed points and their properties tell us which kinds of Γ_k are viable fundamental theories which can be extended to arbitrarily high energy scales. A remarkable feature of this method is that it can predict the values and evolution of interaction couplings, simply by requiring them to flow to the fixed point. This is because the subspace of actions that converge to the fixed point typically has a smaller dimension than the entire space. As a result, requiring convergence to the fixed point fixes coefficients in the set of all actions. It is then only necessary to pinpoint (by experiment) which theory in the smaller subspace is realized.

Assuming we have performed the previous steps and a suitable fixed point is found, we will have found classes of effective actions that are well-defined at arbitrarily high energy scales. From this we might want to reconstruct the path integral and, in particular, the classical action associated with this effective action. This effectively amounts to reversing the process often performed in quantum field theories, where fundamental interactions are given and the effective dynamics due to quantization are to be computed. Due to some features of the functional renormalization group, which we will discuss in more detail in the following chapter, the bare action can indeed be reconstructed from the fixed point Γ_*. At this step, the ultraviolet cutoff we (could have) removed in the evolution equation has to be reintroduced. The specific form of the cutoff, together with the information of the fixed point, determine how the bare action and path integral behave when the ultraviolet cutoff is sent to infinity.

At the level of the effective action physical scenarios can also be studied. One then identifies the scale k with

some physical scale of the system. This scale is related to the energy of the system in some way, for example this can be the temperature in early-universe cosmology. The evolution of the effective action then affects the dynamics of the system by introducing quantum gravity effects. A recent example of this can be found in [7], where asymptotic safety is used to obtain a viable cosmological evolution, from Starobinsky inflation at early times to standard General Relativity with a cosmological constant at late times.

We have largely left out details up to now while discussing the basic ideas of the functional renormalization group. In the following chapters we will go into these details. However not every aspect will be covered, in particular symmetries in the gravitational case. For a more complete discussion, we refer the reader to [1], which a lot of the introduction will be based on.
Currently, the Asymptotic Safety program yields promising results [8]. Various pure gravity models have been studied and found to support the possibility of an asymptotically safe theory of quantum gravity. When adding matter, two major effects are the matter effects on quantum spacetime, and the quantum gravity effects on matter. For the former, in the cases of minimally coupled Standard Model matter fields, studies have found that the asymptotic safety mechanism is also operative in this case. For the latter, there are hints that asymptotically safe quantum gravity might bring about a predictive and observationally viable UV completion for the Standard Model. A degree of caution should be held against these findings, as more work is necessary to provide definitive answers to all questions.

The question this thesis will focus on concerns the choice of regulator which is necessary to define the Effective Average Action Γ_k. In particular we will look into choices of coarse graining operators, which essentially define what high and low energy means in a curved spacetime. Chapters 2 through 5 will introduce the functional renormalization group for gravity and the coarse graining operators. Chapters 6 and 7 constitute original work of this thesis. We first investigate the effect of a change in regulator or coarse graining in the formal machinery of the renormalization group in chapter 6. The results of this analysis are worked out and compared in a simple quantum gravity scenario in chapter 7. In chapter 8 we summarize the results and make suggestions for future calculations which might help suppress unphysical regulator effects due to approximations.

2 Introduction to the Functional Renormalization Group

In applications of quantum field theory, the objective is to calculate expectation values $\langle O \rangle$ of observables O. In a perturbative setting, these are computed by means of Feynman diagrams, and nonperturbatively with the following functional integral

$$\langle O \rangle = C \int Dh\, O(h) e^{-S[h]}. \tag{2.1}$$

Here C is a normalization constant such that $\langle 1 \rangle = 1$, and h is the collection of all quantum fields. In principle this would include the spacetime metric, all known matter fields, all known gauge fields and any nonphysical fields resulting from gauge fixing. In general we will suppress indices of the fields. An important subset of these observables are the n-point functions, which consist of a string of fields $\langle h(x_1)h(x_2)...h(x_n) \rangle$. For these we can write down a generating functional. Introducing a source $J(x)$, which is an element of the dual space of the field configurations $h(x)$, we define the partition function

$$Z[J] \equiv \int Dh\, e^{-S[h]+Jh}. \tag{2.2}$$

The product of J and h in d-dimensional Euclidean spacetime is canonically defined as $Jh \equiv \int \sqrt{g} d^d x J(x)h(x)$. Note that if the theory contains multiple fields, then there is a source J for each field, and the product is between these pairs. The n-point functions can then be computed by taking functional derivates with respect to the source J:

$$\langle h(x_1), h(x_2), ..., h(x_n) \rangle = \frac{\delta^n Z[J]}{\delta J(x_1)\delta J(x_2)...\delta J(x_n)}\bigg|_{J=0}. \tag{2.3}$$

Likewise, the generating functional of all connected n-point functions is given by

$$W[J] \equiv \log[Z[J]]. \tag{2.4}$$

Finally there is a third generating functional known as the effective action, $\Gamma[\chi]$, which is the Legendre-Fenchel transform of $W[J]$. Its variable is the field expectation value $\langle h \rangle$, which is an element of the space dual to the space of sources, and is given by $\chi(x) \equiv \langle h(x) \rangle_J = \delta W[J]/\delta J(x)$. In a slight abuse of notation, we use the same brackets now to indicate connected n-point functions, i.e. J is not set to zero afterwards, and the field expectation value is normalized the same way as in (2.1). In terms of equations, the effective action has the form:

$$\Gamma[\chi] = \sup_J (J\chi - W[J]). \tag{2.5}$$

Here the product $J\chi$ is the same kind as Jh, and the source $J[\chi]$ by formally inverting the relation $\chi = \delta W/\delta J$. It can be shown that the effective action generates all 1-particle irreducible n-point functions by functional differentiation with respect to χ .

All functional integrals up to now have been written down formally. In order to make these well-defined, the implementation of ultraviolet (UV) and infrared (IR) cutoffs is necessary. Since the construction of the renormalization group involves introducing an IR cutoff, one only needs to regularize the UV behaviour. One example of this is replacing the continuous spacetime $\mathbb{R}^d$ with a lattice $\mathbb{Z}^d$, in which the lattice spacing plays the role of the UV cutoff. We will implicitly assume the presence of some regularization method, but continue to use formal continuum notation.

We now introduce the Effective Average Action Γ_k and construct the FRGE, which governs its scale-dependence. In line with Wilson's idea of renormalization, the Effective Average Action depends on at which point we start integrating out momentum modes; the modes which are integrated out will contribute to the couplings. The FRGE controls the dependence of Γ_k on the IR-cutoff scale k. The IR-cutoff will have the form of a momentum dependent mass term added to the action that suppresses fluctuation modes with momentum $p^2 \lesssim k^2$. Thus the construction begins with modifying the path integral such that it includes an additional cutoff term $\Delta_k S[h]$ in the action:

$$Z_k[J] \equiv e^{W_k[J]} \equiv \int Dh\, e^{-S[h]+Jh-\Delta_k S[h]}. \tag{2.6}$$

The factor containing the cutoff action suppresses the IR modes of the field h. Primarily for practical purposes, this term is quadratic in the fluctuation field, so that it has the interpretation of a momentum dependent mass term:

$$\Delta_k S[h] \equiv \frac{1}{2}\int d^d x\; h(x) R_k(\Box) h(x). \tag{2.7}$$

Here $\Box$ is the relevant differential operator, related to p^2 in momentum space, and is required to be a positive semi-definite operator. For example we can take $\Box = -\partial_\mu \partial^\mu$. The positive function $R_k(\Box)$ is called the cutoff function or regulator. There is freedom in its precise form, but for it to be a proper cutoff, it has to satisfy the following properties, in terms of p^2:

- $R_k(p^2) \to 0$ for $k \to 0$. A consequence of this is that we obtain the usual effective action Γ in the limit $k \to 0$.
- $R_k(p^2) \to 0$ sufficiently fast for $p^2 \gg k^2$, so that high momentum modes are not suppressed. Here the meaning of sufficiently fast depends on the spacetime dimension and whether or not the theory contains higher derivative terms.
- $R_k(p^2) \propto k^2$ for $p^2 \lesssim k^2$, such that the low momentum modes acquire a mass of $\mathcal{O}(k)$. This also entails that the regulator diverges for $k \to \infty$, completely suppressing all modes.

This description of a regulator generalizes the idea of suppressing modes below a certain scale by a "smooth" (not necessarily in the mathematical sense) cutoff. An example of a regulator function is the exponential cutoff

$$R_k(p^2) = \frac{p^2}{e^{p^2/k^2}-1}. \tag{2.8}$$

This regulator is not often used in practical calculations because relevant expressions cannot be calculated analytically with this cutoff, making the computation more expensive numerically. However, it has properties which are useful for our analysis later on, namely that it is smooth and nonzero for all finite p and k. Often the cutoffs are expressed in terms of a factor times a dimensionless shape function: $R_k(p^2) = k^2 R^{(0)}(p^2/k^2)$. In the case of an exponential cutoff, the shape function is:

$$R^{(0)}(z) = \frac{z}{e^z - 1}. \tag{2.9}$$

This regulator can be seen as a special case of a 1-parameter family of regulators, given by the shape function

$$R^{(0)}(z;s) = \frac{sz}{e^{sz}-1}, \qquad s > 0. \tag{2.10}$$

The exponential cutoff (2.8) is then the case $s = 1$. This generalization can be seen as (from the perspective of the cutoff) a re-scaling of the spectrum since the 1-parameter family can be acquired by scaling the momentum eigenvalues $p \to \sqrt{s}p$.
The definition of the Effective Average Action (EAA) now follows from the same procedure as the ordinary effective action, but now stemming from the scale dependent path integral (2.6). We define the functional $W_k[J]$ and the connected field expectation value $\chi(x)$ in the same way. The Legendre-Fenchel transform $\hat{\Gamma}_k$ of W_k then gives

$$\hat{\Gamma}_k[\chi] = \sup_J (J\chi - W_k[J]). \tag{2.11}$$

If we can invert the relation $\chi[J]$ for the source, which amounts to solving for the supremum, and find a functional $J = \mathcal{J}_k[\chi]$, the Legendre transform will be given by

$$\hat{\Gamma}_k[\chi] = \mathcal{J}_k[\chi]\chi - W_k[\mathcal{J}_k[\chi]]. \tag{2.12}$$

Note that in this construction both the source and the field expectation value have a k dependence. The Effective Average Action is then defined by [9]

$$\Gamma_k[\chi] \equiv \hat{\Gamma}_k[\chi] - \Delta_k S[\chi]. \tag{2.13}$$

The reason for subtracting the regulator term is that the resulting Γ_k has better properties, especially when we look at the FRGE.

2.1 The Functional Renormalization Group Equation

The objective of Asymptotic Safety is to find a theory which is well-behaved for all scales k, including the UV and IR limits. To accomplish this, we need to know about the behaviour of the effective average action with respect to the energy scale. Clearly then, a cornerstone of this approach is the evolution equation Γ_k obeys, which is called the functional renormalization group equation (FRGE)[3]. Defining $t = \log(k)$ as the renormalization group time, the FRGE states that

$$\partial_t \Gamma_k[\chi] = \frac{1}{2}\mathrm{STr}\left[\left(\frac{\delta^2\Gamma_k}{\delta\chi\delta\chi} + R_k\right)^{-1}\partial_t R_k\right]. \tag{2.14}$$

The operator $\frac{\delta^2\Gamma_k}{\delta\chi\delta\chi}$ is the Hessian of the effective average action, and has matrix elements

$$\frac{\delta^2\Gamma_k}{\delta\chi\delta\chi}(x,y) \equiv \frac{\delta^2\Gamma_k}{\delta\chi(x)\delta\chi(y)}. \tag{2.15}$$

We will derive the FRGE as follows. Regarding k and χ as independent variables, the t derivative of (2.12) is

$$\partial_t \hat{\Gamma}_k[\chi] = -\partial_t W_k[\mathcal{J}_k]. \tag{2.16}$$

[3]The FRGE is also called the Wetterich equation. These two names will be used interchangeably in this thesis.

Inserting definitions (2.6), (2.7) this is found equal to

$$\frac{1}{Z_k[J]}\int dh e^{-S[h]-\Delta S_k[h]+J[h]}\left[\frac{1}{2}\int d^dx h(x)\partial_t R_k(\Box)h(x)\right]=\frac{1}{Z_k[J]}\frac{1}{2}\mathrm{Tr}[\langle hh\rangle^{dc}\partial_t R_k]. \tag{2.17}$$

The expectation value with the superscript dc stands for the disconnected expectation value, without superscript they are connected expectation values. By comparing expressions of the connected and disconnected 2-point functions one can relate them by

$$\frac{1}{Z_k[J]}\langle h(x)h(y)\rangle^{dc}=\frac{\delta^2 W_k}{\delta J(x)\delta J(y)}+\chi(x)\chi(y). \tag{2.18}$$

Using this, the previous expression becomes

$$\partial_t\hat{\Gamma}_k[\chi]=\frac{1}{2}\mathrm{Tr}\big[\frac{\delta^2 W_k}{\delta J\delta J}\partial_t R_k+\langle h\rangle\,\partial_t R_k\,\langle h\rangle\,\big]=\frac{1}{2}\mathrm{Tr}\big[\frac{\delta^2 W_k}{\delta J\delta J}\partial_t R_k\big]+\partial_t\Delta_k S[\chi]. \tag{2.19}$$

The last term on the RHS is the required price for the definition of Γ_k(2.13) from $\hat{\Gamma}_k$. Bringing it to the LHS and using definiton (2.13) gives

$$\partial_t\Gamma_k[\chi]=\frac{1}{2}\mathrm{Tr}\big[\frac{\delta^2 W_k}{\delta J\delta J}\partial_t R_k\big]. \tag{2.20}$$

In order to get to a self consistent equation, we finally eliminate W_k in terms of Γ_k. We first notice that the effective average action obeys

$$\frac{\delta\Gamma_k}{\delta\chi(x)}+R_k(\Box)\chi(x)=J(x). \tag{2.21}$$

This implies

$$\frac{\delta^2 W_k}{\delta J(x)\delta J(y)}=\frac{\delta\chi(x)}{\delta J(y)}=\left[\frac{\delta J(y)}{\delta\chi(x)}\right]^{-1}=\left[\frac{\delta^2\Gamma_k}{\delta\chi(x)\delta\chi(y)}+R_k(x,y)\right]^{-1}. \tag{2.22}$$

Combining (2.20) and (2.22) then results in the FRGE (2.14), where the supertrace sums over all fields with appropriate minus signs for Grassmann fields.

At the level of the FRGE, the aforementioned UV regularization is not necessary anymore. To see this, let us fix k. In the UV, because $R_k(p^2)\to 0$ for $p^2\gg k^2$, the argument of the trace behaves like

$$\left(\frac{\delta^2\Gamma_k}{\delta\chi\delta\chi}+R_k\right)^{-1}\partial_t R_k\sim\left(\frac{\delta^2\Gamma_k}{\delta\chi\delta\chi}(p^2)\right)^{-1}\partial_t R_k(p^2). \tag{2.23}$$

The Hessian, being a two-point function, equals $p^2+...$ in momentum representation, where ... are higher order terms, including both higher derivative and interaction terms. The product then equals

$$(p^2+...)^{-1}\partial_t R_k(p^2). \tag{2.24}$$

Here the meaning of the regulator decaying sufficiently fast becomes relevant; the trace will give an integral over momenta. Assuming there are no higher order momentum terms, $\partial_t R_k(p^2)$ will have to decay faster than $1/p^{d-2}$ for the integral to converge in the UV. The exponential cutoff has an exponential decay in the

UV, so this is guaranteed for any spacetime dimension.
The infrared field modes also give only a finite contribution. To show this we use the fact that $R_k \propto k^2$ for $p^2 \lesssim k^2$. In momentum representation the integrand is then:

$$(\frac{\delta^2\Gamma_k}{\delta\chi\delta\chi} + R_k)^{-1}\partial_t R_k \sim \frac{2k^2}{p^2 + k^2 + ...}. \tag{2.25}$$

Here the limit $p^2 \to 0$ is easily evaluated to be finite and equal to 2 if we ignore the higher order terms.

One might also wonder about the limits of k. When analyzing the FRGE, these limits are taken after the trace is evaluated, i.e. after the aforementioned integration of p. For both limits we will assume to have rewritten the equation with dimensionless spacetime coordinates and fields. This results in both sides having exclusively dimensionless couplings, and k is the only dimensionful quantity left after the momentum integration. Furthermore, because the LHS is a dimensionless derivative of an action, the FRGE is dimensionless. Because the RHS is dimensionless, and k is the only dimensionful quantity, we can conclude that the RHS has no explicit k dependence. All dependence on the RG scale k is implicit in the dimensionless couplings, and the convergence behaviour is dependent only on this. Since on the RHS the couplings appear in the denominator[4] the flow goes to 0 if the couplings diverge. However if we expand the denominator we reach the opposite conclusion: the flow is then infinite when the coupling goes to infinity. Because the convergence of these limits is dictated by the convergence of the couplings, it is closely related to the existence of a fixed point in the UV or IR.

Finally, the FRGE has a diagrammatic expression. Even though the FRGE is an exact equation, it has a one-loop structure. Here $(\Gamma_k'' + R_k)^{-1}$ is the full propagator and is indicated with a line, and a regularization factor $\partial_t R_k$ is indicated with a grey blob. The trace then closes the propagator $(\Gamma_k'' + R_k)^{-1}$ into a regularized loop. The FRGE in diagrammatic notation then looks like

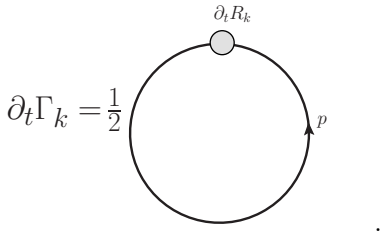

Figure 1: The Wetterich equation in diagrammatic form which has a one-loop structure. The momentum p in the loop is integrated over. The grey blob with $\partial_t R_k$ indicates that this loop is regulated by a factor $\partial_t R_k$.

[4]The regulator might contain some couplings, in particular a wavefunction renormalization is a canonical choice. For the sake of this argument we assume this is not the case.

2.2 Properties of the Effective Average Action

The effective average action satisfies the integro-differential equation:

$$\begin{aligned}\exp\{-\Gamma_k[\chi]\} = \int Dh \exp\left\{-S[h] + \int d^dx (h(x)-\chi(x)) \frac{\delta\Gamma_k}{\delta\chi(x)}\right\} \\ \exp\left\{-\int \frac{1}{2} d^dx (h(x))-\chi(x)) R_k(\Box)(h(x)-\chi(x))\right\}.\end{aligned} \tag{2.26}$$

Its derivation follows from the definitions (2.6) (2.12), (2.13) and the effective field equation (2.21). Exponentiating minus the EAA with (2.12) and (2.13) gives the expression

$$\exp\{-\Gamma_k[\chi]\} = \exp\left\{-\int d^dx\ J(x)\chi(x)\right\} \exp\left\{\frac{1}{2}\int d^dx\ \chi(x) R_k \chi(x)\right\} \exp\{W_k\}. \tag{2.27}$$

Substituting the definition (2.6) for W_k for the last term gives us

$$\begin{aligned}\exp\{-\Gamma_k[\chi]\} = \exp\left\{-\int d^dx\ J(x)\chi(x)\right\} \exp\left\{\frac{1}{2}\int d^dx\ \chi(x) R_k \chi(x)\right\} \\ \int Dh \exp\left\{-S[h] + \int d^dx\ J(x)h(x) - \frac{1}{2}\int d^dx\ h(x) R_k(\Box) h(x)\right\}.\end{aligned} \tag{2.28}$$

For the source $J(x)$ we can substitute the effective field equation (2.21) in (2.28). With some partial integration and ordering of the terms, the result (2.26) is found.

An important property of the EAA that can be studied based on this equation is the $k \to \infty$ limit of Γ_k. Since $R_k \propto k^2$ for $k \to \infty$, the second exponential of the RHS of the equation becomes $\exp\left[-k^2 \int d^dx (\chi(x)-h(x))^2\right]$, which is a delta functional $\delta[\chi - h]$ up to normalization. The integration can then be done to find $\lim_{k\to\infty} \Gamma_k[\chi] = S[\chi]$. The $k \to 0$ limit follows trivially from the definition, so the effective average action has the limits:

$$\boxed{\Gamma \xleftarrow{k\to 0} \Gamma_k \xrightarrow{k\to\infty} S}. \tag{2.29}$$

In this sense the bare action is an initial condition for the FRGE. Otherwise the FRGE is completely independent of the bare action. Based on these limits, the bare action can be reconstructed by integrating the FRGE with some initial condition.

The limits of Γ_k are independent of the choice of the regulator R_k, and if the EAA converges to a fixed point in these limits, then also the fixed point is independent of the regulator. Although the fixed point is unaffected by a regulator change, for finite k the solutions will depend on the regulator. This has the interpretation of a coordinate change in the theory space of solutions of the FRGE. An infinitesimal deformation of the regulator $R_k \to R_k + \delta R_k$ changes the effective average action by

$$\delta\Gamma_k = \frac{1}{2}\mathrm{STr}\left[\left(\frac{\delta^2\Gamma_k}{\delta\chi\delta\chi} + R_k\right)^{-1} \delta R_k\right]. \tag{2.30}$$

This relation is formally derived in the same way as the FRGE: the ∂_t derivative is replaced by the deformation δ in (2.16), (2.17) and one then follows the same steps to this result. This can be seen as a generalization of the FRGE, as we can insert an infinitesimal change in t for the deformation, which gives $R_k \to R_k + \partial_t R_k$, and recover the Wetterich equation. Because $R_k + \delta R_k$ is also a regulator, δR_k needs to have the same falloff behaviour as a regulator. This means that the same steps we used for the FRGE can be used to show the

convergence of this trace.

3 Asymptotic Safety

3.1 Theory Space and Truncations

We will now discuss the space of solutions of the FRGE. Because the effective action functionals have similar complexity as the path integral, this space is large and complicated. The solutions to the FRGE live in what we call theory space $\mathcal{T}$, which should contain all possible action functionals. We define theory space by the following requirements:

- All functionals $A[\cdot] \in \mathcal{T}$ are invariant under the relevant symmetry transformations. In gravity these transformations are diffeomorphisms. Otherwise they are given by the corresponding gauge group.
- Theory space contains all functionals that can occur in a derivative expansion, i.e. arbitrary field monomials, consisting of any number of fields and derivatives acting on them in all possible ways[5].

The monomials I_α then act as a basis of $\mathcal{T}$. For example these can be of the form $(\partial_\mu\chi\cdot\partial^\mu\chi)^q$ or $\chi^p(\partial_\mu\chi\cdot\partial^\mu\chi)^q$. An arbitrary element $A[\chi]$ of theory space will then look like

$$A[\chi] = \sum_\alpha \bar{u}^\alpha I_\alpha[\chi], \tag{3.1}$$

where $I_\alpha[\chi]$ is an element of this basis, and the $\bar{u}^\alpha$ are the couplings (coupling constants) of these monomials. In general these will have a nonzero canonical dimension. If a coupling $\bar{u}^\alpha$ has a canonical mass dimension q_α, its dimensionless counterpart is defined as

$$u^\alpha = \bar{u}^\alpha k^{-q_\alpha}. \tag{3.2}$$

These dimensionless couplings and their behaviour in the RG flow are of primary interest to us. Their scale derivatives are called the beta functions:

$$\beta_\alpha(u(t)) = \partial_t u^\alpha = k\partial_k u^\alpha. \tag{3.3}$$

When expressed in terms of dimensionless couplings, the beta functions do not have an explicit k dependence, because k is the only dimensionful quantity remaining. We can move to a dimensionless theory space by moving the extra power of k to the fields and expressing our functionals in terms of these dimensionless fields. We shall do this implicitly here, which makes it so that we only work with dimensionless quantities, and the factor k^{-q} originating from the canonical dimension goes away.
Since the couplings can be seen as the coefficients for the basis expansion of an element $A[\chi]$, there is an obvious one-to-one correspondence between a set of couplings $\{u^\alpha\}$ and an element of theory space $A[\chi]$. Given that the EAA is an element of $\mathcal{T}$, we can write the FRGE as follows

$$\sum_\alpha k\partial_k u^\alpha(k) I_\alpha[\chi] = \frac{1}{2}\,\mathrm{Tr}\left[\left(k^2\sum_\alpha u^\alpha(k) I''_\alpha[\chi] + R_k\right)^{-1} k\partial_k R_k\right]. \tag{3.4}$$

[5] One can extend this by also including terms which have no derivative expansion, e.g. $u_i \exp\{1/\chi^2\}$.

Here $I''_\alpha[\chi]$ is the second functional derivative of the monomial $I_\alpha[\chi]$. The factor k^2 arises because of the implicit change in fields; in (3.4) we take the functional derivative with respect to a dimensionless field as opposed to a dimensionful field in (2.14). Because of the complexity of this non-linear functional equation, and the fact it is in principle an infinite series, we must resort to some kind of approximation. A perturbative expansion, where couplings are assumed small, is a possibility. However we will resort to an approximation at the level of theory space. This has the advantage of resulting in non-perturbative approximate solutions. While the series may be finite similarly as in perturbation theory, in principle contributions from all orders of the coupling constants are summed. They may also include terms non-analytic in the couplings, which do not appear in standard perturbation theory.

The basic idea of the approximation is to project the differential equation (3.4) onto a simpler, usually finite subspace $\mathcal{T}_{trunc} \subset \mathcal{T}$. Working on this subset entails two assumptions, which we shall clarify with by example of an N-dimensional subset $\mathcal{T}_{trunc}$. For this to be a good approximation we need that

$$\sum_\alpha k\partial_k u^\alpha(k) I_\alpha[\chi] = \sum_{i=1}^{N} k\partial_k u_i(k) I_i[\chi]. \tag{3.5}$$

As is obvious from this equation, the approximation includes assuming that $u^\alpha \to 0$ for $I_\alpha[\chi] \notin \mathcal{T}_{trunc}$, or if not zero, in some sense small. The second assumption can be seen from the FRGE on the truncated space, which would state that

$$\sum_{i=1}^{N} \partial_k u^i(k) I_i[\chi] = \frac{1}{2}\,\mathrm{Tr}\left[\left(k^2 \sum_{i=1}^{N} u^i(k) I''_i[\chi] + R_k\right)^{-1} \partial_k R_k\right]. \tag{3.6}$$

Even though only the monomials I_i belonging to the truncated space appear in the trace, the derivative expansion of these will generate terms outside of $\mathcal{T}_{trunc}$ because of the inverse propagator and second derivative of the monomials. Since the RHS generates terms which are supposed to equal the scale derivative of couplings outside the truncated subspace, we have to assume these beta functions to be zero (or small) as well: $\partial_k u^\alpha \to 0$ when $I_\alpha \notin \mathcal{T}_{trunc}$.

This can also be seen from the first argument: to have the equality (3.5) at the level of functions of k, the assumption $u^\alpha \to 0$ needs to hold for all k, which implies that the scale derivative of u^α is likewise small or zero. Essentially, we are allowed to set the coupling to zero at some k_0, as this would simply correspond to setting initial conditions. However, this coupling will in general be generated by the RG flow at different scales k. We will need to apply a projection on the FRGE to restrict this to the truncation space $\mathcal{T}_{trunc}$. Ignoring the generating of this coupling is the real approximation step and the reason why a projection of the FRGE is an approximation. Since the coupling that would be generated also, in general, influences the RG flows of the couplings living in the truncation subspace, the results regarding even this small subset of couplings are also not exact. This can be illustrated as viewing projecting the EAA and solving the FRGE as non-commuting: an exact solution to the projected FRGE is not equal to a projected solution of the exact FRGE.

A point we want to stress is that these arguments hold for every aspect of the FRGE that is formally derived. We argued that (3.6) is an approximation to the exact FRGE (2.14). For the same reason, other formal results, which exactly hold for the exact FRGE and its solutions, are broken by the projection of the FRGE onto a truncation space. In particular this refers to the deformation described by (2.30), the integro-differential equation (2.26), as well as formal results from chapters further in the thesis. For the

same reason, when methods will be compared later on, we do not really have a formal basis to claim which result is correct. The accuracy of an equation or method in the approximation has to be judged by expanding the truncation space and seeing if physical results are stable[6]. This is to say, even though the FRGE is the most widely used tool in this field, it does not have a different status than the methods which will be developed and tested in chapters 6 and 7.

3.2 Fixed points

Fixed points are important points in (dimensionless) theory space, characterized by the property that they do not evolve under the RG flow. It is therefore a point $u_* = u_*^\alpha$ for which all beta functions are zero:

$$\beta_\alpha(u_*) = 0 \quad \forall\, \alpha. \tag{3.7}$$

The existence of a fixed point is important because it implies trajectories of the RG flows that converge to some finite point in theory space, i.e. theories that are well-defined, without physical divergences, for all RG scales k. Whether or not such a fixed point exists and what its properties are is a highly nontrivial question, since the fixed point condition is an infinite set of coupled algebraic equations. This can be reduced to a finite set in a truncation, but it will generally retain a lot of complexity. Our definitions will distinguish two kinds of fixed points: Gaussian and non-Gaussian fixed points (GFP and NGFP respectively). Gaussian fixed points correspond to free field theories i.e. the RG flow in the vicinity of a Gaussian fixed point behaves like the RG flow of a free theory. Non-Gaussian fixed points have some nonzero interactions. While the dimensionless couplings are scale independent at this fixed point, the dimensionful couplings still have a k-dependence:

$$\bar{u}^\alpha(k) = u_*^\alpha k^{q_\alpha}. \tag{3.8}$$

Here q_α is the canonical mass dimension of $\bar{u}^\alpha$. Notably, the dimensionful couplings do diverge in the UV limit even when the theory approaches or sits at the fixed point. The assumption that gravity has a non-Gaussian fixed point which is the UV limit of a subset of theory space is called the Asympotic Safety Conjecture or Asymptotic Safety Scenario. When the UV limit of a theory is Gaussian it is called asymptotically free. We shall see that a fixed point can imply a great deal of predictability for Asymptotic Safety and asymptotic freedom.

3.2.1 Linearized flow

We also want to know about the behaviour of RG trajectories that stay close to the fixed point for some time without being on the fixed point at all times. For this we linearize the beta functions at the fixed point u_*^α. This results in the system of linear differential equations,

$$\partial_t u^\alpha = \sum_\mu B_\mu^\alpha (u^\mu - u_*^\mu), \tag{3.9}$$

where B_μ^α are the components of the stability matrix B of the fixed point:

$$B_\mu^\alpha = \frac{\partial}{\partial u^\mu} \beta^\alpha(u)\big|_{u=u_*}. \tag{3.10}$$

[6]It can also be judged, of course, by comparing to experiments. This is rather tricky when concerning quantum gravity; the energy scale of quantum gravity effects lies far beyond what can be currently probed by experiments.

We assume[7] that this matrix admits a complete set of right eigenvectors V_n satisfying

$$BV_n = -\theta_n V_n. \tag{3.11}$$

The numbers θ_n which are minus the eigenvalues are called the critical exponents of the fixed point. Since in general B is not symmetric they are complex numbers. Their significance is best seen when writing down the general solution of the linearized RG equation:

$$u^\alpha(k) = u^\alpha_* + \sum_n C_n V_n^\alpha (\frac{k_0}{k})^{\theta_n}. \tag{3.12}$$

Here the C_n are integration constants and k_0 is a fixed reference scale. From this equation we can see that UV attractive directions correspond to $\mathrm{Re}(\theta_n) > 0$ and UV repulsive (IR attractive) directions correspond to $\mathrm{Re}(\theta_n) < 0$. The vectors associated with these critical exponents are called relevant or irrelevant respectively. If the real part is zero then the direction is called marginal. In order for the flow to approach the fixed point in the UV, the C_n of the irrelevant directions have to be zero so as to not diverge with increasing k, while the contributions of the relevant directions approach the fixed point for increasing k. Likewise the marginal directions differ from the fixed point by a finite number in the UV limit if their C_n are nonzero[8]. Hence the dimension of the subspace that converges to the NGFP for $k \to \infty$ is given by the number of nonzero C_n, which corresponds to the number of critical exponents θ_n with $\mathrm{Re}(\theta_n) > 0$. This is called the UV critical hypersurface, its dimension indicates how many independent measurements need to be made to determine which theory living in the UV critical hypersurface is realized in Nature. The Asymptotic Safety scenario is therefore more predictive the smaller the dimensionality of the UV critical hypersurface is.
Using the critical exponents we can give a precise definition of Gaussian and non-Gaussian fixed points. Free field theories have critical exponents equal to their canonical mass dimensions. The flow in the vicinity of the fixed point then behaves like the flow of a free theory if and only if the critical exponents are equal to the canonical mass dimensions of the couplings. We therefore define that a fixed point is Gaussian if all its critical exponents are equal to the canonical mass dimensions of the couplings, and non-Gaussian if this is not the case. This definition has the advantage of being coordinate independent; even if the action might not look like a free theory at the fixed point, this definition gives a straightforward way to check this.

[7] This assumptions turns out to be correct in all RG investigations of quantum gravity so far.
[8] This is assuming the imaginary part is nonzero. If the imaginary part is also zero, one needs to go beyond the linear term.

4 The Functional Renormalization Group for Gravity

We have now constructed the Effective Average Action (EAA) and its Functional Renormalization Group. In this chapter we will discuss some additional aspects of the FRGE specific to gravity, which will later become relevant when applying this methods to pure gravity. The discussion will be limited to what is necessary for us, namely the Fadeev-Popov gauge fixing procedure, and the background field method, and is thus not exhaustive. For a more complete picture we refer the reader to [1]. In this chapter and the later chapter on the application to gravity we will restore internal indices.

4.1 The Background Field Method

In order to avert problems arising when attempting to construct a quantum field theory of gravity, such as the fact that a quantum field theory is constructed on an already fixed spacetime, we approach the problem by means of the background field method[12, 13]. In the background field method we decompose the dynamical metric $\widehat{g}_{\mu\nu}$ into a classical background metric $\bar{g}_{\mu\nu}$ and a dynamical quantum field $\widehat{h}_{\mu\nu}$. The EAA will then be a functional of both fields. $\bar{g}_{\mu\nu}$ will describe the background spacetime structure and $\widehat{h}_{\mu\nu}$ describes the quantized degrees of freedom which are integrated over in the path integral. Together they make the full spacetime metric. This can be parametrized in different ways, two possibilities are the linear split and exponential split:

$$\widehat{g}_{\mu\nu} = \bar{g}_{\mu\nu} + \widehat{h}_{\mu\nu}, \tag{4.1}$$

$$\widehat{g}_{\mu\nu} = \bar{g}_{\mu\rho}(e^{\widehat{h}})^{\rho}_{\nu}. \tag{4.2}$$

Because the degrees of freedom are distributed differently in these parametrizations, it might be that this choice amounts to quantizing different physical theories. In a way, one can interpret the resulting theory as a (spin 2) matter field on a given classical spacetime, for which the inverse metric and covariant derivative are well-defined. To restore background independence and get a full quantum field theory of gravity we must repeat the quantization of $\widehat{h}_{\mu\nu}$ for all backgrounds $\bar{g}_{\mu\nu}$, giving an interpretation of a quantum gravity theory as an infinite number of standard quantum field theories of matter on a given classical spacetime. The raising and lowering of indices is then done with the background metric and quantities constructed from the background metric indicated with a bar, e.g. $D(\bar{g}_{\mu\nu}) = \bar{D}, R(\bar{g}_{\mu\nu}) = \bar{R}$.
In line with the previous construction we can define the effective average action in the background field formalism. We equip the path integral over the fluctuation field with an IR regulator. In order to retain the structure of the FRGE (2.14) and in line with the interpretation of quantizing a matter field $\widehat{h}_{\mu\nu}$ in a spacetime described by the metric $\bar{g}_{\mu\nu}$, the cutoff action only works on the fluctuation fields:

$$\Delta_k S^{\text{grav}}[\widehat{h}; \bar{g}] = \frac{\kappa^2}{2} \int d^d x \sqrt{\bar{g}}\, \widehat{h}_{\mu\nu} R_k^{\text{grav}}[\bar{g}]^{\mu\nu\rho\sigma} \widehat{h}_{\rho\sigma}. \tag{4.3}$$

Here κ is a constant with the dimension of a mass necessary so that the action is dimensionless, we shall usually set $\kappa = (32\pi G)^{-\frac{1}{2}}$ for this and other arbitrary mass constants, where G is the measured reference value of Newton's constant. Otherwise the derivation of the effective average action and FRGE is conceptually the same, with the addition of contributions originating from gauge fixing, which we will discuss now.

4.2 Gauge Fixing and Ghost Fields

A cornerstone of General Relativity is diffeomorphism invariance, often called invariance under general coordinate transformations. The diffeomorphisms[9] act on the metric with the Lie derivative with respect to a generating vector field v^μ:

$$\delta\widehat{g}_{\mu\nu} = \mathcal{L}_v\widehat{g}_{\mu\nu} = v^\rho\partial_\rho\widehat{g}_{\mu\nu} + \partial_\mu v^\rho\widehat{g}_{\rho\nu} + \partial_\nu v^\rho\widehat{g}_{\rho\mu}. \tag{4.4}$$

Just like quantum field theories with a gauge symmetry group, General Relativity has the group of diffeomorphisms as its symmetry group. Similarly to gauge theories, the contribution of unphysical gauge degrees of freedom must be regularized in the path intergal, leading to a gauge fixing and ghost action. We start off with path integral of the form

$$\int D\widehat{g}_{\mu\nu}e^{-S[\widehat{g}_{\mu\nu}]+J^{\mu\nu}\widehat{h}_{\mu\nu}}, \tag{4.5}$$

which, like before, is implicitly regularized in the UV, and $J^{\mu\nu}$ is the source associated with the metric. Using the linear split (4.1), we can instead integrate over $\widehat{h}_{\mu\nu}$, since $\bar{g}_{\mu\nu}$ is a fixed background metric. We now want to rewrite this as a functional integral which integrates only over physically inequivalent field configurations. The gauge transformations we have to gauge fix are the so-called quantum gauge transformation δ^Q, which act according to (4.4) and do not change $\bar{g}_{\mu\nu}$:

$$\delta^Q\widehat{h}_{\mu\nu} = \mathcal{L}_v\widehat{g}_{\mu\nu} = \mathcal{L}_v(\bar{g}_{\mu\nu} + \widehat{h}_{\mu\nu}), \qquad \delta^Q\bar{g}_{\mu\nu} = 0. \tag{4.6}$$

Choosing a gauge fixing function $F_\mu(\widehat{h}, \bar{g})$, the well-known Faddeev-Popov trick can be applied[10, 20, 21, 22, 23]. The functional integral then becomes

$$\int D\widehat{h}_{\mu\nu}DC^\mu D\bar{C}_\mu e^{-S[\widehat{h}+\bar{g}]-S_{\text{gf}}[\widehat{h};\bar{g}]-S_{\text{gh}}[\widehat{h},C,\bar{C};\bar{g}]}. \tag{4.7}$$

The first extra term is the gauge fixing action S_{gf}, which is of the general form

$$S_{\text{gf}}[\widehat{h};\bar{g}] = \frac{1}{2\gamma}\int d^dx\ \sqrt{\bar{g}}\ \bar{g}^{\mu\nu}F_\mu(\widehat{h};\bar{g})F_\nu(\widehat{h};\bar{g}). \tag{4.8}$$

The gauge fixing function is arbitrary for now, as well as the gauge fixing parameter γ. We shall specify the choice of gauge fixing function later. The second additional term S_{gh}, along with the new integration variables $C^\mu, \bar{C}_\mu$ is the contribution of the Faddeev-Popov ghosts and anti-ghosts. The ghost action also depends on the gauge fixing function

$$S_{\text{gh}}[\widehat{h}, C, \bar{C}; \bar{g}] = -\kappa^{-1}\int d^dx\ \sqrt{\bar{g}}\ \bar{C}_\mu\bar{g}^{\mu\nu}\frac{\partial F_\nu}{\partial\widehat{h}_{\alpha\beta}}\mathcal{L}_C(\widehat{h}_{\alpha\beta} + \bar{g}_{\alpha\beta}). \tag{4.9}$$

Here the mass scale κ appears again, we will set it to the same value of $(32\pi G)^{-\frac{1}{2}}$ as before. The ghost fields are anticommuting vector fields, and therefore not physical. The ghost action S_{gh} has the ghost kinetic operator $\mathcal{M}$ and is acquired in the usual way: first the gauge transformation δ^Q is applied to F_μ, the result is contracted with $\bar{C}_\mu$ and finally the parameters v^μ are replaced by the anticommuting field C^μ[24]. The Faddeev-Popov determinant is then exponentiated by functional integration over the ghosts C^μ and

[9] More precisely, the diffeomorphisms generated by vector fields, which is a small subset in a mathmatical sense, see [15].

antighosts $\bar{C}_\mu$:

$$\det[\mathcal{M}] = \det\left[\frac{\delta^Q F_\mu}{\delta v^\nu}\right] = \int DC^\mu D\bar{C}_\mu e^{-\sqrt{2}\int d^dx\ \sqrt{\bar{g}}\ \bar{C}_\mu \mathcal{M}^\mu{}_\nu C^\nu}. \tag{4.10}$$

After using the gauge fixing condition $F_\mu[\widehat{h}, \bar{g}] = 0$, the effective action constructed from the gauge fixed path integral is no longer invariant under the quantum transformation δ^Q. After all, this is the very reason for the gauge fixing procedure. However, the functionals are still invariant under the special class of background gauge transformations δ^B, defined by

$$\delta^B \widehat{h}_{\mu\nu} = \mathcal{L}_v \widehat{h}_{\mu\nu}, \qquad \delta^B \bar{g}_{\mu\nu} = \mathcal{L}_v \bar{g}_{\mu\nu}. \tag{4.11}$$

This definition implies $\delta^B F_\mu = \mathcal{L}_v F_\mu$, and therefore the bare action and gauge fixing action are invariant under background gauge transformations:

$$\delta^B S[\bar{g} + \widehat{h}] = 0 = \delta^B S_{\text{gf}}[\widehat{h}; \bar{g}]. \tag{4.12}$$

The full metric transforms in the same manner as (4.4) for both the quantum transformations δ^Q and background transformations δ^B. However, these transformations distribute the variation of $\widehat{g}_{\mu\nu}$ differently over $\bar{g}_{\mu\nu}$ and $\widehat{h}_{\mu\nu}$. The quantum transformations keep $\bar{g}_{\mu\nu}$ unchanged and works only on the fluctuation field $\widehat{h}_{\mu\nu}$, while the background transformations change both $\widehat{h}_{\mu\nu}$ and $\bar{g}_{\mu\nu}$ with their own Lie derivative. For every choice of $F_\mu[\widehat{h}; \bar{g}]$, the ghost fields transform in the same way as the metric with respect to the background transformations:

$$\delta^B C^\mu = \mathcal{L}_v C^\mu, \qquad \delta^B \bar{C}_\mu = \mathcal{L}_v \bar{C}_\mu. \tag{4.13}$$

So like before, the ghost action is also invariant under background gauge transformations. Together with (4.11), we can therefore conclude that the total action, including gauge fixing and ghost terms, is invariant under background gauge transformations:

$$\delta^B(S[\bar{g} + \widehat{h}] + S_{\text{gf}}[\widehat{h}; \bar{g}] + S_{\text{gh}}[\widehat{h}, C, \bar{C}; \bar{g}]) = 0. \tag{4.14}$$

This will allow us to set up an EAA that is fully invariant under background transformations δ^B. Furthermore each field has a source which is introduced in the usual way.

There are many choices for the gauge fixing function, a convenient choice which we will use is linear in the fluctuation field and belongs to the one-parameter family of generalized harmonic gauge conditions:

$$\begin{aligned} F_\mu &= \sqrt{2}\kappa \mathcal{F}_\mu^{\alpha\beta}[\bar{g}]\widehat{h}_{\alpha\beta}, \\ \mathcal{F}_\mu^{\alpha\beta} &= \delta_\mu^\beta \bar{g}^{\alpha\gamma}\bar{D}_\gamma - \omega \bar{g}^{\alpha\beta}\bar{D}_\mu. \end{aligned} \tag{4.15}$$

Here ω is a free parameter. Note that the covariant derivative $\bar{D}_\mu$ is constructed from the background metric. The ghost kinetic operator for this choice of gauge condition is

$$\mathcal{M}[\widehat{g}, \bar{g}]^\mu_\nu = \bar{g}^{\mu\rho}\bar{g}^{\sigma\lambda}\bar{D}_\lambda(\widehat{g}_{\rho\nu}D_\sigma + \widehat{g}_{\sigma\nu}D_\rho) - 2\omega\bar{g}^{\rho\sigma}\bar{g}^{\mu\lambda}\bar{D}_\lambda \widehat{g}_{\sigma\nu}D_\rho, \tag{4.16}$$

so the ghost action reads

$$S_{\text{gh}}[\widehat{h}, C, \bar{C}; \bar{g}] = -\sqrt{2}\int d^dx\ \sqrt{\bar{g}}\ \bar{C}_\mu \mathcal{M}^\mu{}_\nu C^\nu. \tag{4.17}$$

Furthermore, the ghost fields are also suppressed by the cutoff action, which has a similar form as the gravitational part:

$$\Delta_k S^{\rm gh}[C,\bar{C};\bar{g}] = \sqrt{2}\int d^dx\ \sqrt{\bar{g}}\ \bar{C}_\mu R_k^{\rm gh}[\bar{g}]C^\mu. \tag{4.18}$$

The prefactor $\sqrt{2}$ is chosen to match the prefactor in the ghost action. We can then construct the effective average action for gravity in the usual way, with as arguments field expectation values $h = \langle\widehat{h}\rangle\,, g = \langle\widehat{g}\rangle\,, \bar{g} = \langle\bar{g}\rangle\,, \xi = \langle C\rangle\,, \bar{\xi} = \langle\bar{C}\rangle$. The general form of the FRGE (2.14) still holds, in which the supertrace gives two contributions from the anticommuting ghosts with a minus sign.

4.3 Split symmetry and the Ward identity

When discussing the background field method, we saw two different ways of splitting the full metric in a background and fluctuation field (4.1), (4.2). Obviously, there are infinitely many ways to do this split. In the case of the linear split for example, the full metric $g_{\mu\nu}$ is invariant under the split symmetry transformations

$$\delta\widehat{h}_{\mu\nu} = \epsilon_{\mu\nu}, \qquad \delta\bar{g}_{\mu\nu} = -\epsilon_{\mu\nu}. \tag{4.19}$$

Since we start out with an action that depends only on the full metric $\widehat{g}_{\mu\nu} = \widehat{h}_{\mu\nu} + \bar{g}_{\mu\nu}$, these objects are also invariants under this transformation. However, as can be seen from (4.3), (4.15), this invariance is broken by the gauge fixing and the regulator which depend on the fields $\widehat{h}$ and $\bar{g}$ separately and not in the combation $\widehat{h} + \bar{g} = \widehat{g}$. The extra dependence on the background $\bar{g}$ of the effective average action is governed by the modified Ward identity for the split symmetry[26]:

$$\frac{\delta\Gamma_k}{\delta\bar{g}_{\mu\nu}} = \frac{1}{2}{\rm STr}\left[\left(\frac{\delta^2\Gamma_k}{\delta\widehat{h}\delta\widehat{h}} + R_k\right)^{-1}\frac{\delta S''_{\rm tot}}{\delta\bar{g}_{\mu\nu}}\right]. \tag{4.20}$$

Here $S''_{\rm tot}$ is the Hessian of the total bare action

$$S''_{\rm tot} \equiv \frac{\delta^2}{\delta\widehat{h}\delta\widehat{h}}\left(S[\bar{g}+\widehat{h}] + S_{\rm gf}[\widehat{h};\bar{g}] + S_{\rm gh}[\widehat{h},C,\bar{C};\bar{g}] + \Delta_k S[\widehat{h},C,\bar{C};\bar{g}]\right), \tag{4.21}$$

which is dependent on the background field $\bar{g}$ outside of the combination $\bar{g}+\widehat{h}$ because of the coarse graining operator $\Delta_k S'' = R_k[\bar{g}]$ and the gauge fixing sector. For exact RG trajectories this modified Ward identity and the FRGE are consistent, but this consistency may be broken in truncations.

4.4 The Einstein-Hilbert truncation

The previous analysis considered only the exact case, which means the FRGE is a set of infinitely many differential equations. The step from this full theory to a truncation of it causes previously established exact results to no longer be realized due to the approximation. In particular the choice of regulator affects the fixed point, in contrast with what we conclude from (2.29). This is not surprising, since the approximation may spoil cancellations which would preserve certain properties. It is therefore important to investigate the previous results in truncations to see how they are affected. We will opt for an effective average action of single-metric Einstein-Hilbert form and, as a precursor to later chapters, have coarse graining operators $\Box = -D^2 + \alpha_s\bar{R}$ parametrized by the numbers α_s, where s indicates the spin of the fields. These results will be compared to other methods in the chapter 7.

For the purpose of this analysis we will take a relatively simple truncation, namely the single-metric Einstein-Hilbert truncation in $d = 4$ dimensional spacetime. This means that we take the gravitational part of the effective average action to be of Einstein-Hilbert form: $\Gamma_k^{\text{grav}}[g, \bar{g}] = \bar{\Gamma}_k[g] + \widehat{\Gamma}_k[g, \bar{g}] = \frac{1}{16\pi G_k} \int d^4x\sqrt{g}(-R + 2\Lambda_k) + \widehat{\Gamma}_k[g, \bar{g}]$. The background and fluctuation field will be seperated by a linear split (4.1). The bi-metric part is then set to either 0 or of the form of the gauge-fixing part of the action. We will choose the latter to simplify the algebra, i.e. $\widehat{\Gamma}_k[g, \bar{g}] = \gamma(\frac{G}{G_k} - \frac{1}{\gamma})S_{\text{gf}}$, where G is a k-independent reference value of Newton's constant and γ is the gauge fixing parameter. Finally the gauge fixing and ghost contributions are of the k-independent form (4.8), (4.17). This choice of truncation then leads to the following form of the effective average action[10]:

$$\Gamma_k[g, \bar{g}, \xi, \bar{\xi}] = \Gamma_k^{\text{grav}}[g, \bar{g}] + S_{\text{gf}}[g - \bar{g}; \bar{g}] + S_{\text{gh}}[g - \bar{g}, \xi, \bar{\xi}; \bar{g}]. \tag{4.22}$$

For the gauge fixing we will choose the standard harmonic (de Donder) gauge, i.e. $\omega = 1/2$ in (4.15):

$$F_\mu[h; \bar{g}] = \sqrt{2}\kappa(\bar{D}^\nu h_{\mu\nu} - \frac{1}{2}\bar{D}_\mu \bar{g}^{\rho\gamma} h_{\rho\gamma}). \tag{4.23}$$

Where $\kappa = (32\pi G)^{-1/2}$ is the same constant mass parameter as before, and h is the fluctuation field. Barred operators and quantities are defined with respect to the background metric $\bar{g}$. We will also choose $\gamma = 1$. Additionally, instead of working with the Newton constant G_k, we will work with a dimensionless coupling $Z_k = G/G_k$. The complete truncation ansatz for Γ_k is then as follows:

$$\begin{aligned}\Gamma_k[g, \bar{g}, \xi, \bar{\xi}] = {} & 2\kappa^2 Z_k \int d^4x\sqrt{g}(-R + 2\Lambda_k) \\ & + \kappa^2 Z_k \int d^4x\sqrt{\bar{g}}\bar{g}^{\mu\nu}(\bar{D}^\alpha h_{\mu\alpha} - \frac{1}{2}\bar{D}_\mu \bar{g}^{\alpha\beta} h_{\alpha\beta})(\bar{D}^\rho h_{\nu\rho} - \frac{1}{2}\bar{D}_\mu \bar{g}^{\rho\gamma} h_{\rho\gamma}) + S_{\text{gh}}[g - \bar{g}, \xi, \bar{\xi}; \bar{g}].\end{aligned} \tag{4.24}$$

We can now put this into the FRGE. After performing the derivates with respect to the metric we can set $\bar{g}_{\mu\nu} = g_{\mu\nu}$. The LHS then reads

$$\partial_t \Gamma_k[g, g] = 2\kappa^2 \int d^4x\sqrt{g}[-R\partial_t Z_k + 2\partial_t(Z_k\Lambda_k)]. \tag{4.25}$$

For the RHS we need to compute the second functional derivative of the effective average action. We can then set the background and fluctuation metric equal and compare the coefficients of powers of R with the LHS to find the beta functions for Z_k and Λ_k. For the ghost sector the Hessian is the ghost kinetic operator (4.16). We can then expand the remaining part $\Gamma_k[g, \bar{g}] \equiv \Gamma_k^{\text{grav}} + S_{\text{gf}}$ as

$$\Gamma_k[g, \bar{g}] = \Gamma[\bar{g}, \bar{g}] + \mathcal{O}(h) + \frac{1}{2}\Gamma_k^{\text{quad}}[h; \bar{g}] + \mathcal{O}(h^3). \tag{4.26}$$

We can then read off the Hessian from Γ^{quad},

$$\Gamma_k^{\text{quad}}[h; \bar{g}] = 2Z_k\kappa^2 \int d^4x\sqrt{\bar{g}} h_{\mu\nu}[-K^{\mu\nu}{}_{\rho\sigma}\bar{D}^2 + U^{\mu\nu}{}_{\rho\sigma}]h^{\rho\sigma}, \tag{4.27}$$

[10] We have omitted the BRST variations, as they are not relevant to the discussion and we have skipped over them in the previous sections.

where the tensors K, U are given by

$$K^{\mu\nu}{}_{\rho\sigma} = \frac{1}{4}[\delta^\mu_\rho\delta^\nu_\sigma + \delta^\mu_\sigma\delta^\nu_\rho - \bar{g}^{\mu\nu}\bar{g}_{\rho\sigma}], \tag{4.28}$$

$$\begin{aligned} U^{\mu\nu}{}_{\rho\sigma} = &\frac{1}{4}[\delta^\mu_\rho\delta^\nu_\sigma + \delta^\mu_\sigma\delta^\nu_\rho - \bar{g}^{\mu\nu}\bar{g}_{\rho\sigma}](\bar{R} + 2\Lambda_k) + \frac{1}{2}[\bar{g}^{\mu\nu}\bar{R}_{\rho\sigma} + \bar{g}_{\rho\sigma}\bar{R}^{\mu\nu}] \\ &- \frac{1}{4}[\delta^\mu_\rho\bar{R}^\nu{}_\sigma + \delta^\mu_\sigma\bar{R}^\nu{}_\rho + \delta^\nu_\rho\bar{R}^\mu{}_\sigma + \delta^\nu_\sigma\bar{R}^\mu{}_\rho] - \frac{1}{2}[\bar{R}^\nu{}_\rho{}^\mu{}_\sigma + \bar{R}^\nu{}_\sigma{}^\mu{}_\rho]. \end{aligned} \tag{4.29}$$

Now we want to diagonalize this quadratic form, the first part of this diagonalization is the decomposition of $h_{\mu\nu}$ in a traceless tensor $\mathring{h}_{\mu\nu}$ and a trace part ϕ. This has the form

$$h_{\mu\nu} = \mathring{h}_{\mu\nu} + \frac{1}{4}\bar{g}_{\mu\nu}\phi, \quad \bar{g}^{\mu\nu}\mathring{h}_{\mu\nu} = 0, \quad \phi = \bar{g}^{\mu\nu}h_{\mu\nu} \tag{4.30}$$

Expressed in these fields, (4.27) is given by

$$\Gamma_k^{\text{quad}}[h;\bar{g}] = 2Z_k\kappa^2\int d^4x\sqrt{\bar{g}}\Big[\frac{1}{2}\mathring{h}_{\mu\nu}(-\bar{D}^2 - 2\Lambda_k + \bar{R})\mathring{h}^{\mu\nu} - \frac{1}{8}\phi(-\bar{D}^2 - 2\Lambda_k)\phi \tag{4.31}$$

$$- \bar{R}_{\mu\nu}\mathring{h}^{\nu\rho}\mathring{h}^\mu{}_\rho + \bar{R}_{\rho\sigma\mu\nu}\mathring{h}^{\sigma\nu}\mathring{h}^{\rho\mu}\Big] \tag{4.32}$$

Further we exploit the freedom of Background Independence. This allows us to choose a maximally symmetric space as our background. This implies the following relations between the Riemann and Ricci tensor, and the Ricci scalar (in 4 spacetime dimensions)

$$\begin{aligned} \bar{R}_{\mu\nu\rho\sigma} &= \frac{1}{12}(\bar{g}_{\mu\rho}\bar{g}_{\nu\sigma} - \bar{g}_{\mu\sigma}\bar{g}_{\nu\rho})\bar{R}, \\ \bar{R}_{\mu\nu} &= \frac{1}{4}\bar{g}_{\mu\nu}\bar{R}. \end{aligned} \tag{4.33}$$

For a maximally symmetric background the quadratic part then takes the form

$$\Gamma_k^{\text{quad}}[h;\bar{g}] = Z_k\kappa^2\int d^4x\sqrt{\bar{g}}\Big[\mathring{h}_{\mu\nu}(-\bar{D}^2 - 2\Lambda_k + \frac{2}{3}\bar{R})\mathring{h}^{\mu\nu} - \frac{1}{4}\phi(-\bar{D}^2 - 2\Lambda_k)\phi\Big] \tag{4.34}$$

Since the derivates have all been resolved, we can now set $\bar{g} = g$, so the bars on metric dependent quantities will be omitted from now on. We also need the Faddeev-Poppov operator for the ghost fields. Because of our gauge fixing condition it is the same as (4.16), and at $\bar{g} = g$ is given by

$$\mathcal{M}^\mu_\nu = \delta^\mu_\nu D^2 + R^\mu_\nu = -\delta^\mu_\nu(-D^2 - \frac{1}{4}R). \tag{4.35}$$

The last equality is a result of using a maximally symmetric background. We now have all second derivatives in a completely diagonal form as necessary for the trace on the RHS of the FRGE. Next, we need to specify how the cutoff works on the different fields. Each cutoff term has the structure

$$R_k[\bar{g}] = \mathcal{Z}_k k^2 R^{(0)}(\frac{\Box}{k^2}), \tag{4.36}$$

where the prefactor $\mathcal{Z}_k$ is chosen such that the modified propagator is proportional to $(\Box + k^2R^{(0)})$. The coarse graining operator $\Box$ is chosen to be $\Box = -\bar{D}^2 + \alpha_s\bar{R}$. The real endomorphism parameters α_s appear here, where its subscript (s for spin) will indicate on which field (tensor "T", scalar "S" or vector "V") it

acts. From (4.34) we can see that the traceless and trace parts differ by a prefactor of $-1/4$, which suggests the following:

$$\begin{aligned}(\mathcal{Z}_k)_{\mathring{h}\mathring{h}} &= Z_k,\\ (\mathcal{Z}_k)_{\phi\phi} &= -\frac{1}{4}Z_k,\\ (\mathcal{Z}_k)_{\xi\bar{\xi}} &= 1.\end{aligned} \tag{4.37}$$

Because we neglect renormalization effects in the ghost sector, the prefactor for the ghost regulator is simply 1. The final form of the propagators then read, at $\bar{g} = g$

$$\begin{aligned}(\kappa^{-2}\Gamma_k''[g,g] + R_k)_{\widehat{h}\widehat{h}} &= Z_k\left[-D^2 + k^2 R^{(0)}(\frac{-D^2+\alpha_T R}{k^2}) - 2\Lambda_k + \frac{2}{3}R\right],\\ (\kappa^{-2}\Gamma_k''[g,g] + R_k)_{\phi\phi} &= -\frac{1}{4}Z_k\left[-D^2 + k^2 R^{(0)}(\frac{-D^2+\alpha_S R}{k^2}) - 2\Lambda_k\right],\\ (-\mathcal{M} + R_k)_{\xi\bar{\xi}} &= \left[-D^2 + k^2 R^{(0)}(\frac{-D^2+\alpha_V R}{k^2}) - \frac{1}{4}R\right].\end{aligned} \tag{4.38}$$

With this we have the ingredients we need to compute the RHS of the FRGE. Inserting (4.38) in (2.14) and accounting for the contributions with the supertrace gives

$$\partial_t\Gamma_k[g,g] = \mathrm{Tr}_T[\mathcal{N}_T(\mathcal{P}_T + (\frac{2}{3}-\alpha_T)R)^{-1}] + \mathrm{Tr}_S[\mathcal{N}_S(\mathcal{P}_S - \alpha_S R)^{-1}] - 2\,\mathrm{Tr}_V[\mathcal{N}_V^{(0)}(\mathcal{P}_V^{(0)} - (\frac{1}{4}+\alpha_V)R)^{-1}], \tag{4.39}$$

with the operators

$$\begin{aligned}\mathcal{P}_s &\equiv (-D^2 + \alpha_s R) + k^2 R^{(0)}(\frac{-D^2+\alpha_s R}{k^2}) - 2\Lambda_k\\ \mathcal{N}_s &\equiv (2Z_k)^{-1}\partial_t[Z_k k^2 R^{(0)}(\frac{-D^2+\alpha_s R}{k^2})]\\ &= [1 - \frac{1}{2}\eta]k^2 R^{(0)}(\frac{-D^2+\alpha_s R}{k^2}) + (D^2 - \alpha_s R)R^{(0)\prime}(\frac{-D^2+\alpha_s R}{k^2}).\end{aligned} \tag{4.40}$$

The prime denotes the derivative with respect to the argument, and η is the anomalous dimension of Newton's constant $\eta \equiv -\partial_t \ln Z_k$. The subscript once again indicates on which type of field the operator acts, and the $\mathcal{P}^{(0)}, \mathcal{N}^{(0)}$ are defined like (4.40) but with $\Lambda_k = 0, Z_k = 1, \eta_k = 0$. The factor $\frac{1}{2}$ in front of the trace in the FRGE is absorbed into $\mathcal{N}_s$

Because our truncation ansatz is of first order in the curvature scalar, we can expand these traces in powers of R

$$\begin{aligned}\partial_t\Gamma_k[g,g] = {}& \mathrm{Tr}_T[\mathcal{N}_T\mathcal{P}_T^{-1}] + \mathrm{Tr}_S[\mathcal{N}_S\mathcal{P}_S^{-1}] - 2\,\mathrm{Tr}_V[\mathcal{N}_V^{(0)}\mathcal{P}_V^{(0)-1}]\\ &- R\left((\frac{2}{3}-\alpha_T)\,\mathrm{Tr}_T[\mathcal{N}_T\mathcal{P}_T^{-2}] - \alpha_S\,\mathrm{Tr}_S[\mathcal{N}_S\mathcal{P}_S^{-2}] + 2(\frac{1}{4}+\alpha_V)\,\mathrm{Tr}_V[\mathcal{N}_V^{(0)}\mathcal{P}_V^{(0)-2}]\right) + \mathcal{O}(R^2).\end{aligned} \tag{4.41}$$

Note that we view the combination $(-D^2 + \alpha_s R)$ as a variable independent of the theory space basis element R. Because it is the chosen coarse graining operator we will integrate over this quantity. We can evaluate

these traces with heat kernel methods[11]. For a generic function W with Fourier transform $\widetilde{W}$, the expansion of the trace is given by (in 4 spacetime dimensions)

$$\mathrm{Tr}_s[W(\Box)] = (4\pi)^{-2}\,\mathrm{tr}_s(I)\left[Q_2[W]\int d^4x\sqrt{g} + Q_1[W]\int d^4x\sqrt{g}(\frac{1}{6}R - \mathbf{E}) + \mathcal{O}(R^2)\right]. \tag{4.42}$$

Here the I stands for the unit matrix on the space of fields, and the small trace tr is a trace only over internal indices, so $\mathrm{tr}_s[I]$ is the number of independent field components. In our case these equal

$$\begin{aligned}\mathrm{tr}_S[I] &= 1,\\ \mathrm{tr}_V[I] &= 4,\\ \mathrm{tr}_T[I] &= 9.\end{aligned} \tag{4.43}$$

Furthermore $\mathbf{E}$ stands for the endomorphism we use in $\Box = -D^2 + \mathbf{E}$ as the argument of W, i.e. $\mathbf{E} = \alpha_s R$ in this computation. Finally we have introduced functionals

$$Q_n[W] \equiv \int_{-\infty}^{\infty} ds(-is)^{-n}\widetilde{W}(s). \tag{4.44}$$

Here $\widetilde{W}(s)$ is the Fourier transform of the function $W(z)$. In terms of the original function $W(z)$, for positive n, these equal

$$Q_n[W] = \frac{1}{\Gamma(n)}\int_0^{\infty} dz\; z^{n-1}W(z). \tag{4.45}$$

We will now evaluate the traces in (4.41) as the RHS of the flow equation and compare them with the LHS of the flow equation (4.25). Then comparing the coefficient of the $\sqrt{g}$ term gives us:

$$\partial_t(Z_k\Lambda_k) = \frac{1}{4\kappa^2}\frac{1}{(4\pi)^2}\left[9Q_2[\mathcal{N}_T/\mathcal{P}_T] + Q_2[\mathcal{N}_S/\mathcal{P}_S] - 8Q_2[\mathcal{N}_V^{(0)}/\mathcal{P}_V^{(0)}]\right], \tag{4.46}$$

and comparing the coefficient for the $\sqrt{g}R$ term gives

$$\begin{aligned}\partial_t Z_k = -\frac{1}{12\kappa^2}\frac{1}{(4\pi)^2}\Bigg[&9\left((1-6\alpha_T)Q_1[\mathcal{N}_T/\mathcal{P}_T] - 6(\frac{2}{3}-\alpha_T)Q_2[\mathcal{N}_T/\mathcal{P}_T^2]\right)\\ &+\left((1-6\alpha_S)Q_1[\mathcal{N}_S/\mathcal{P}_S] + 6\alpha_S Q_2[\mathcal{N}_S/\mathcal{P}_S^2]\right)\\ &-8\left((1-6\alpha_V)Q_1[\mathcal{N}_V^{(0)}/\mathcal{P}_V^{(0)}] + 6(\frac{1}{4}+\alpha_V)Q_2[\mathcal{N}_V^{(0)}/\mathcal{P}_T^{(0)2}]\right)\Bigg].\end{aligned} \tag{4.47}$$

Here in (4.47) we have ordered the lines by their spin. The $\mathcal{N}$ and $\mathcal{P}$ are considered as functions of the argument $z = -D^2 + \alpha_s R$. Because of this, the α dependence is no longer present in the integration due to substitution, i.e. $Q_n[\mathcal{N}_S/\mathcal{P}_S] = Q_n[\mathcal{N}_T/\mathcal{P}_T]$ etc., and the spin subscript of $\mathcal{N}$ and $\mathcal{P}$ no longer matters.

[11] See Appendix A for a brief exposition on the heat kernel expansion.

It is now convenient to introduce normalized, dimensionless threshold functions:

$$\Phi_n^p(\omega) \equiv \frac{1}{\Gamma(n)} \int_0^\infty dz\ z^{n-1} \frac{R^{(0)}(z) - zR^{(0)\prime}(z)}{(z + R^{(0)}(z) + \omega)^p}, \tag{4.48}$$

$$\widetilde{\Phi}_n^p(\omega) \equiv \frac{1}{\Gamma(n)} \int_0^\infty dz\ z^{n-1} \frac{R^{(0)}(z)}{(z + R^{(0)}(z) + \omega)^p}. \tag{4.49}$$

Here p and n are integers with $p \geq 1, n \geq 0$. The integration is over the dimensionless argument $z = \frac{-D^2 + \alpha R}{k^2}$. In terms of these dimensionless threshold functions, (4.46) becomes

$$\partial_t(Z_k \Lambda_k) = (4\kappa^2)^{-1}(4\pi)^{-2} k^4 \Big[10\Phi_2^1(\frac{-2\Lambda_k}{k^2}) - 8\Phi_2^1(0) - 5\eta\tilde{\Phi}_2^1(\frac{-2\Lambda_k}{k^2}) \Big]. \tag{4.50}$$

Likewise, (4.47) becomes

$$\begin{aligned} \partial_t Z_k = -(24\kappa^2)^{-1}(4\pi)^{-2} k^2 \Big[& (20 - 108\alpha_T - 12\alpha_S)(\Phi_1^1(\frac{-2\Lambda_k}{k^2}) - \frac{1}{2}\eta\tilde{\Phi}_1^1(\frac{-2\Lambda_k}{k^2})) \\ & - (72 - 108\alpha_T - 12\alpha_S) \left(\Phi_2^2(\frac{-2\Lambda_k}{k^2}) - \frac{1}{2}\eta\tilde{\Phi}_2^2(\frac{-2\Lambda_k}{k^2}) \right) \\ & - (16 - 96\alpha_V)\Phi_1^1(0) - (24 + 96\alpha_V)\Phi_2^2(0) \Big]. \end{aligned} \tag{4.51}$$

We will want to switch to dimensionless coupling constants. The RG scale k has the dimension of a mass, and gives a natural mass scale with which we can define dimensionless couplings:

$$g_k = k^2 G_k = k^2 Z_k^{-1} \bar{G}, \quad \lambda_k = k^{-2} \Lambda_k \tag{4.52}$$

From the previous equation we get the flow of the dimensionless newton constant:

$$\beta_g \equiv \partial_t g_k = [2 + \eta] g_k \tag{4.53}$$

An implicit equation for η can be found from (4.51)

$$\eta = g_k B_1^{\mathrm{FRGE}}(\lambda_k, \alpha_s) + \eta g_k B_2^{\mathrm{FRGE}}(\lambda_k, \alpha_s) \tag{4.54}$$

The function $B_1^{\mathrm{FRGE}}, B_2^{\mathrm{FRGE}}$ are given by

$$\begin{aligned} B_1^{\mathrm{FRGE}}(\lambda_k, \alpha_s) = \frac{1}{3}(4\pi)^{-1} \Big[& (20 - 108\alpha_T - 12\alpha_S)\Phi_1^1(-2\lambda_k) - (72 - 108\alpha_T - 12\alpha_S)\Phi_2^2(-2\lambda_k) \\ & - (16 - 96\alpha_V)\Phi_1^1(0) - (24 + 96\alpha_V)\Phi_2^2(0) \Big] \\ B_2^{\mathrm{FRGE}}(\lambda_k, \alpha_s) = -\frac{1}{3}(4\pi)^{-1} \Big[& (10 - 54\alpha_T - 6\alpha_S)\tilde{\Phi}_1^1(-2\lambda_k) - (36 - 54\alpha_T - 6\alpha_S)\tilde{\Phi}_2^2(-2\lambda_k) \Big] \end{aligned} \tag{4.55}$$

The superscript FRGE is added with the other methods in mind, they will give similar equations with different B functions. The distinction will be made with these superscripts. Solving (4.54) for η then gives

$$\eta(g_k, \lambda_k) = \frac{g_k B_1^{\mathrm{FRGE}}(\lambda_k, \alpha_s)}{1 - g_k B_2^{\mathrm{FRGE}}(\lambda_k, \alpha_s)} \tag{4.56}$$

The scale derivative of the dimensionless cosmological constant is related to the previous expressions by

$$\beta_\lambda \equiv \partial_t \lambda_k = -(2-\eta)\lambda_k + 32\pi g_k \kappa^2 k^{-4} \partial_t (Z_k \Lambda_k) \tag{4.57}$$

Which gives us the beta function for the cosmological constant:

$$\beta_\lambda = -(2-\eta)\lambda_k + 2g_k(4\pi)^{-1}\Big[10\Phi_2^1(-2\lambda_k) - 8\Phi_2^1(0) - 5\eta\tilde{\Phi}_2^1(-2\lambda_k)\Big] \tag{4.58}$$

We can see that the general form of the beta functions (4.53), (4.58) is independent of our choices of $\alpha_T, \alpha_S, \alpha_V$: all dependence of these parameters is in the anomalous dimension η. The flow of the couplings then depend on the coarse graining through η. The beta functions are in agreement with the literature [11] when we set all $\alpha_s \to 0$.

These beta functions, or alternatively (4.51), (4.50); and their dependence on α, will be the basis of the analysis. This will be the benchmark against which the other formally exact results will be tested. This comparison can be made at the level of the beta functions. However, a more straightforward (and perhaps more physically relevant) quantitative comparison can be made by looking at the fixed points and their properties.

4.4.1 Fixed point analysis

Let us return to the system of RG equations (4.53), (4.58). We will search for fixed point coordinates in the $g\lambda$-plane of theory space. The fixed point has coordinates (g_*, λ_*) such that both of the beta functions are zero:

$$\begin{aligned} \beta_g(g_*, \lambda_*) &= [2 + \eta(g_*, \lambda_*)]g = 0, \\ \beta_\lambda(g_*, \lambda_*) &= 0. \end{aligned} \tag{4.59}$$

Both conditions are trivially satisfied at the Gaussian fixed point (GFP), where $g_* = 0$ and $\lambda_* = 0$. Furthermore, the first condition is also realized if $\eta = -2$, which we will use to simplify the search for the non-Gaussian fixed point (NGFP). Using this with (4.54) we can solve for g_* as a function of λ_*:

$$g_*(\lambda_*) = \frac{2}{2B_2^{\mathrm{FRGE}}(\lambda_*, \alpha_s) - B_1^{\mathrm{FRGE}}(\lambda_*, \alpha_s)}. \tag{4.60}$$

Using this relation we can eliminate the g-dependence in β_λ at the NGFP, so then we have to solve

$$\beta_\lambda(g_*(\lambda_*), \lambda_*) = 0. \tag{4.61}$$

Because of the complexity of the beta function, this is solved numerically. The threshold functions (4.48), (4.49) are calculated with the exponential cutoff (2.9). It is as this point where we will set all α_s equal:

$$\alpha \equiv \alpha_S = \alpha_T = \alpha_V. \tag{4.62}$$

This amounts to studying only this line in the 3-dimensional parameter space. This is mainly done for simplicity; in many calculations these will be given different values. Furthermore, $\Box = -\bar{D}^2 + \alpha_s \bar{R}$ needs to be a positive semi-definite operator so that we do not have field modes with negative kinetic energy. For a

given background, one can then compute the lowest eigenvalue of the Laplacian Δ, resulting in a bound on admissible values for α, since the lowest eigenvalue[12] of $\Box$ has to be at least zero. Using the spectrum of the Laplacian on a spherical background [2, 16] we will sketch these bounds when $\bar{g}$ describes a spherical metric, for which in 4 dimensions the curvature is related to the radius by

$$\frac{1}{r^2} = \frac{\bar{R}}{12}. \tag{4.63}$$

This procedure restricts the values of α_s with the following lower bounds, keeping in mind that our tensor fields are traceless:

$$\begin{aligned} \alpha_T &\geq -1/6, \\ \alpha_S &\geq 0, \\ \alpha_V &\geq -7/12. \end{aligned} \tag{4.64}$$

Furthermore, from (4.39) we can extract an upper bound for the values of α_s. This is because the denominators should be free of poles on the support of $\Box$. These poles would later be removed by expanding this denominator in powers of the curvature, but we argue that the approximate solutions should ultimately have an extension to the exact case, and therefore it makes sense to require this. We can look at the regime of small p^2 (which here is the eigenvalue of $\Box$) compared to k^2. In this case, one can write the denominator proportional to the form $(1 - 2\lambda_k + (c - \alpha)\frac{\bar{R}}{k^2})$, where k is still arbitrary. In order to avoid poles in the integration, we must have $\alpha \leq c$ [13]. The resulting bounds of this procedure are

$$\begin{aligned} \alpha_T &\leq 2/3, \\ \alpha_S &\leq 0, \\ \alpha_V &\leq -1/4. \end{aligned} \tag{4.65}$$

We can combine the two bounds to find the region of admissible values for α_s:

$$\begin{aligned} \alpha_T &\in [-1/6, 2/3], \\ \alpha_S &= 0, \\ \alpha_V &\in [-7/12, -1/4]. \end{aligned} \tag{4.66}$$

In particular, a nonzero value for α_V is *necessary* in order to fulfill both requirements. When we examine the line (4.62) where all α_s are equal the admissible values need to be smaller than $-1/4$ but larger than $-1/6$, which is impossible. Therefore setting all α_s equal leads the interval of admissible values disappearing. However, due to the truncation and how the calculation is done, in particular the expansion from (4.39) to (4.40), the poles are no longer visible, so it is seemingly unproblematic to cross the bounds given by (4.65). Hence the results are not plagued by a divergence of a denominator in (4.39), but also do not support an extension to the exact flow anymore. With this, we forgo a more general study in favour of having to work only in a 1-dimensional parameter space. We shall look at a wide range of values, which anyhow would be outside of this range. For a general manifold the spectrum of the Laplacian is still an open question.

[12] In some cases the lowest or some of the lowest eigenmodes need to be excluded from the traces, in these cases the lowest relevant eigenvalue takes over this role. This was necessary in [2] because of the transverse-traceless decomposition of the tensor field $h_{\mu\nu}$. Because we have used a simpler field decomposition where we split only the traceless and trace part of $h_{\mu\nu}$, in our truncation this only applies to the ghosts.

[13] A type II coarse graining in the literature refers to α exactly on this bound. Because this removes all curvature dependence in the denominators, it has the advantage of making the calculation easier.

Certainly one could demand that all $\alpha \geq 0$ in order to guarantee positive semi-definiteness of $\Box$, but as can be seen in the spherical case, this can be quite removed from the actual bounds. If we were to do this with the vectors, the upper bound (4.65) would make it so no interval is left.
After imposing (4.62) we can solve (4.61) numerically to find the fixed point coordinates. For $\alpha = 0$ we find the fixed point coordinates $(\lambda_*, g_*) = (0.3590, 0.2723)$. The fixed point coordinates and critical exponents have been computed for $\alpha \in [-2, 2]$ and are shown in figure 2 and table 1.

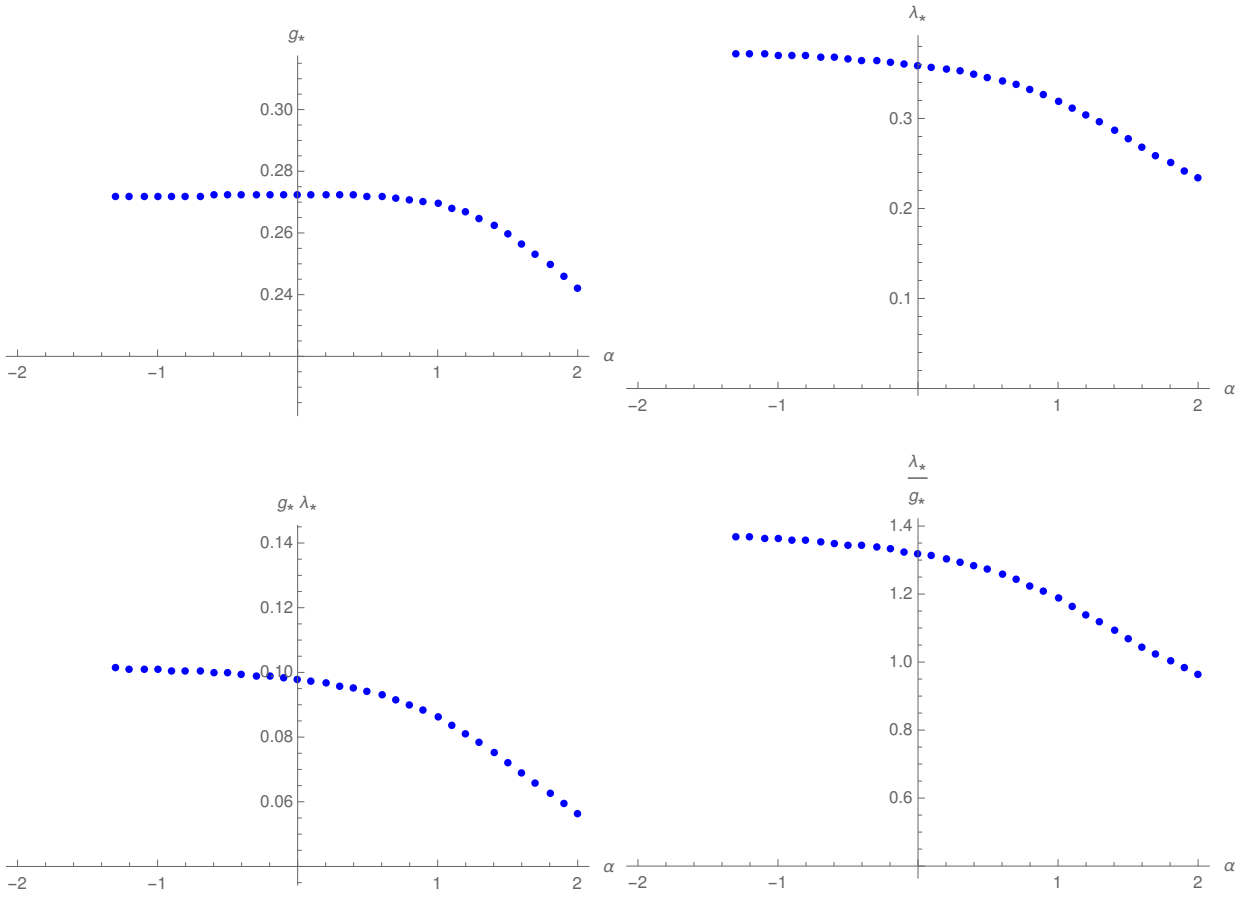

Figure 2: Fixed point coordinates for the FRGE, for values of α from -2 to 2. Around $\alpha \simeq -1.4$ the fixed point vanishes and appears again with negative g_* and λ_* when $\alpha \lesssim -1.4$. These fixed points are not plotted.

Curiously, the fixed point is stable when α exceeds the bounds on either side, and only vanishes around $\alpha \simeq -1.4$, after which the fixed point is restored in the negative (g_*, λ_*) quadrant. The negative fixed points are not included in the plot so that the scale is such that we can distinguish the positive fixed point values. In particular, a negative g_* is unphysical because a negative g_k can not pass to a positive g_k, since the beta function (4.53) can be expanded as $\beta_g = 2g + \mathcal{O}(g^2)$. It is therefore disconnected from the classical regime where g_k is measured to be positive. The product $g_*\lambda_*$ and the fraction $\frac{\lambda_*}{g_*}$ are also far removed from the regular values, so they are not plotted either. Furthermore, the UV critical hypersurface for these negative fixed points is qualitatively different. As can be seen from table 1, there is only 1 critical exponent with positive real part and therefore its critical hypersurface is 1 dimension lower.

Other than the destruction and re-emergence of the fixed point, the results are very stable with respect to variations in α. One can see that the fixed point coordinates only really significantly change for $|\alpha| > 1$, at which point we should begin to question whether the truncation is suitable for these values, since α is

always paired with the scalar curvature R, higher values of α would also more strongly generate terms with higher powers of the curvature. Finally, because the stability matrix components of the fixed point are all real-valued, the two critical exponents are either of the form $a \pm bi$ or are both real.

α	θ_n	λ_*	g_*
-2.0	$(6.8846, -1.8692)$	-0.40121	-1.61705
-1.9	$(7.25695, -1.50051)$	-0.43540	-1.91281
-1.8	$(7.77376, -1.14514)$	-0.47780	-2.34844
-1.7	$(8.57047, -0.798321)$	-0.53317	-3.06807
-1.6	$(10.0989, -0.450919)$	-0.61329	-4.56984
-1.5	$(18.0846, -0.059729)$	-0.79010	-13.5077
-1.4	–	–	–
-1.3	$1.00795 \pm 5.63965i$	0.37258	0.27187
-1.2	$1.03082 \pm 5.5632i$	0.37200	0.27190
-1.1	$1.05475 \pm 5.48337i$	0.37137	0.27194
-1.0	$1.07982 \pm 5.39995i$	0.37069	0.27197
-0.9	$1.10614 \pm 5.3127i$	0.36996	0.27201
-0.8	$1.13380 \pm 5.22135i$	0.36916	0.27205
-0.7	$1.16293 \pm 5.12564i$	0.36828	0.27209
-0.6	$1.19365 \pm 5.02528i$	0.36733	0.27212
-0.5	$1.22612 \pm 4.91994i$	0.36628	0.27216
-0.4	$1.26051 \pm 4.8093i$	0.36512	0.27220
-0.3	$1.29701 \pm 4.693i$	0.36384	0.27223
-0.2	$1.33584 \pm 4.57071i$	0.36242	0.27226
-0.1	$1.37725 \pm 4.44205i$	0.36083	0.27228
0	$1.42153 \pm 4.30669i$	0.35904	0.27230
0.1	$1.46901 \pm 4.16432i$	0.35703	0.27230
0.2	$1.52005 \pm 4.01469i$	0.35475	0.27228
0.3	$1.57504 \pm 3.85768i$	0.35215	0.27223
0.4	$1.63444 \pm 3.69335i$	0.34918	0.27215
0.5	$1.69868 \pm 3.522i$	0.34578	0.27200
0.6	$1.7682 \pm 3.34432i$	0.34187	0.27178
0.7	$1.84338 \pm 3.16151i$	0.33737	0.27146
0.8	$1.92444 \pm 2.97535i$	0.33221	0.27099
0.9	$2.01134 \pm 2.7883i$	0.32634	0.27033
1.0	$2.1037 \pm 2.60338i$	0.31972	0.26942
1.1	$2.20071 \pm 2.42397i$	0.31234	0.26821
1.2	$2.30113 \pm 2.25331i$	0.30430	0.26666
1.3	$2.40343 \pm 2.0941i$	0.29570	0.26472
1.4	$2.50599 \pm 1.94803i$	0.28670	0.26239
1.5	$2.60731 \pm 1.81572i$	0.27748	0.25968
1.6	$2.70615 \pm 1.69684i$	0.26823	0.25663
1.7	$2.80173 \pm 1.59033i$	0.25907	0.25328
1.8	$2.89344 \pm 1.4948i$	0.25014	0.24970
1.9	$2.98108 \pm 1.40874i$	0.24150	0.24593
2.0	$3.06459 \pm 1.33065i$	0.23320	0.24203

Table 1: Critical exponents and fixed point coordinates for the FRGE fixed points. Entries with a $-$ are values of α for which no fixed point was found. Critical exponents are written down as a 2-tuple when both are real, and are of the form $a \pm bi$ otherwise.

These results will be the benchmark against which we will compare other methods. We will now expand on the coarse graining operator $\Box$ and return to these results for the comparison.

5 Coarse graining operators

In this chapter we will focus on different choices of coarse graining operator $\Box$ whose effect on the Functional Renormalization Group is the main study of this thesis. These coarse graining operators are of the general form $\Box = -D^2 + \mathbf{E}$, where $\mathbf{E}$ is an endomorphism on the field space, i.e. it maps fields to fields while retaining their characteristics. In the previous chapter these endomorphisms were exclusively of the form $\alpha_s R\mathbf{1}$. We shall motivate this form and also show generalizations. For coarse graining operators of fermionic fields in particular we will discuss their origin, interpretation, and effect, since in this case they have the most straightforward physical interpretation. For higher spin fields the discussion will be motivated more by mathematics.

5.1 Dirac fermions and the Lichnerowicz formula

When we consider choosing a coarse graining operator, we tend to value "natural" operators, in the sense that they generally appear in the mathematical structure, such as in the Lagrangian or the equations of motion. Every field will have a natural operator in the form of the Laplacian $\Delta = -D_\mu D^\mu$. Dirac spinors have another one which is the Dirac operator. It appears in the Dirac Lagrangian [27]

$$\mathcal{L} = i\bar{\psi}\not{D}\psi + m\bar{\psi}\gamma^5\psi. \tag{5.1}$$

Here the Feynman slash notation is used. The operator of interest is $\not{D}$, or rather $-\not{D}^2$ for the purpose of coarse graining. It appears naturally in the kinetic part of the fermionic action as the contraction of the covariant derivative with the Dirac matrices γ^μ, which are defined by the following anticommutation relation:

$$\{\gamma^\mu, \gamma^\nu\} = 2g^{\mu\nu}\mathbb{1}. \tag{5.2}$$

Using this, together with the first Bianchi identity, the well-known Lichnerowicz formula [17, 18] can be derived:

$$-\not{D}^2 = \Delta + \frac{1}{4}R. \tag{5.3}$$

The Lichnerowicz formula is a first motivation to examine endomorphisms $\mathbf{E}$ proportional to the scalar curvature. Dirac fermions also seem to be most strongly affected by these coarse graining operators. We will show an example of this where a choice in endomorphism parameter α dictates whether or not the theory is asymptotically safe. We will consider the Einstein-Hilbert truncation taken from [2][14], and include only N_D Dirac fermions as matter fields, which are the only fields coarse grained by a coarse graining operator with nonzero α. This means that the truncation ansatz is similar to the one in the previous chapter, but now includes free fermions and has different gauge fixing conditions. Previously we chose the de Donder gauge condition $\gamma = 1$ and $\omega = 1/2$ in (4.8) and (4.15), while now the physical gauge $\gamma = 0$, $\omega \to -\infty$ is chosen. Furthermore, instead of a linear split (4.1) employed in chapter 4, the exponential split (4.2) is now chosen. Finally, regulator function R_k used is a Litim-type regulator [25], i.e.

$$R_k(p^2) = (k^2 - p^2)\theta(k^2 - p^2). \tag{5.4}$$

This regulator is commonly used and allows one to calculate the dimensionless threshold functions (4.48), (4.49) analytically. The beta functions then share a similar general form as before. In particular, the beta

[14] Due to different conventions, there is a difference of sign of α between this thesis and the paper.

α regime	The resulting theory
$\alpha < \alpha_{\text{crit}}$	is asymptotically safe
$\alpha = \alpha_{\text{crit}}$	is divergent for $k \to \infty$
$\alpha > \alpha_{\text{crit}}$	contains a Landau Pole

Table 2: Qualitative conclusions for different values of α.

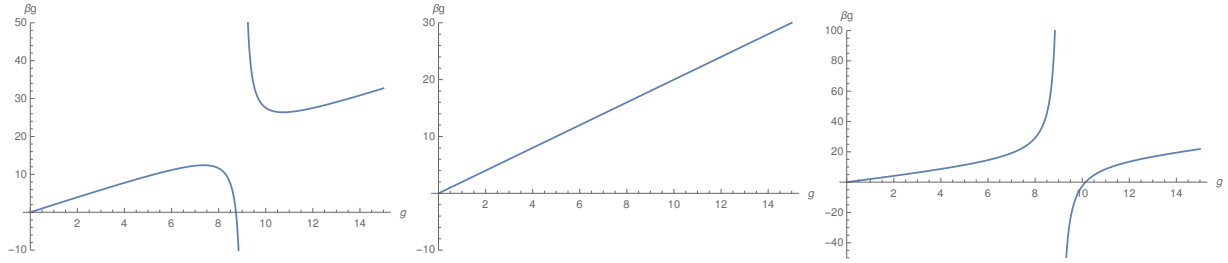

$\alpha < \alpha_{\text{crit}}$ $\alpha = \alpha_{\text{crit}}$ $\alpha > \alpha_{\text{crit}}$

Figure 3: Beta function of the dimensionless Newton constant in the three regimes, since the x-axis represents g and the y-axis represents the change in g, we can see that the fixed point of the left figure is UV attractive, while the fixed point on the right is UV repulsive. Furthermore, the UV repulsive fixed point is also disconnected from the Gaussian fixed point due to the Landau Pole.

function for the dimensionless Newton constant g is as follows:

$$\beta_g = (2 + \eta)g. \tag{5.5}$$

Where the anomalous dimension $\eta = \partial_t \ln(g)$ is again of the form

$$\eta = \frac{gB_1(\alpha)}{1 - gB_2(\alpha)}. \tag{5.6}$$

Now B_1 and B_2 are λ-independent functions depending on the coarse graining parameter. This independence on a cosmological constant is due to the interplay of the exponential split and the physical gauge condition. The B functions are acquired in a similar manner as in chapter 4, substituting them gives the resulting beta function for g:

$$\beta_g = 2g - 3g^2 \frac{43 + 8(1 - 6\alpha)N_D}{72\pi - 25g}. \tag{5.7}$$

The 43 originates from gravitational contributions, while the term proportional to N_D is from Dirac fermions. For large N_D the matter dominates the behaviour of the beta-function. We can see that the value of α drastically influences the sign of higher order terms; the second term can be expanded in a geometric series in powers of g. The terms quadratic and higher in g will either all have positive coefficient, all have negative coefficient, or all vanish, qualitatively altering the asymptotic behaviour of the theory, as shown in table 2 and fig 3, where the beta function β_g is plotted as a function of g. The RG flow is either asymptotically safe in the UV, divergent in the UV; or divergent at finite k, depending on α. The value for which this behaviour changes is

$$\alpha_{\text{crit}} = \frac{43 + 8N_D}{48N_D}, \tag{5.8}$$

which for 1 fermion is $\frac{17}{16}$, for the Standard Model matter content (45/2 Dirac fermions) is approximately 0.206, and for an infinite number of Dirac fermions it is $\frac{1}{6}$. In particular, this means that for the Standard

Model matter content, choosing $\Box = \Delta$ or $\Box = \not{D}^2$, gives an asymptotically safe theory or a theory with a Landau Pole respectively.

The qualitative dependence of this physically relevant result on a *choice* of coarse graining operator is a strong motivation to investigate endomorphisms like these. Evidently, we get different physical theories by changing α, but other than judging by the result, we have no way to discern these values of α as anything special. Presumably, this truncation does not contain the terms necessary in order to compensate for terms generated by the endomorphism $\alpha\bar{R}$. A prescription for choosing coarse graining operators that does not rely on the result of a computation similar to the one shown is necessary. At the end of this chapter we will look at one such prescription.

5.2 Higher integer spins and Lichnerowicz Laplacians

On a (semi-)Riemannian manifold the ordinary Laplacian constructed from the Levi-Civita connection is one possible definition of the Laplacian working on tensor fields. Although it is a straightforward choice, it does not have the most convenient properties, such as respecting symmetries of the tensors it acts on.
The Lichnerowicz Laplacians are generalized from a natural definition of a Laplacian on differential forms (antisymmetric covariant tensors), we will follows the introduction of this in [19]. On these forms the differential d maps the p forms to $p+1$ forms by

$$(d\omega)_{\mu_1\dots\mu_{p+1}} = (p+1)\partial_{[\mu_1}\omega_{\mu_2\dots\mu_{p+1}]}. \tag{5.9}$$

Here the square brackets indicate antisymmetrization with weight one of the indices. With the usual inner product of p forms on a Riemannian manifold, we can define the adjoint δ of d, called the codifferential by

$$d\omega \cdot \beta = \omega \cdot \delta\beta. \tag{5.10}$$

Note that the RHS is an inner product of $p-$forms while the LHS is an inner product of $p+1$-forms. So the codifferential δ maps $p+1$-forms to p-forms, in coordinates the action is given by

$$(\delta\beta)^{\mu_1\dots\mu_p} = -\frac{1}{\sqrt{g}}\partial_\lambda(\sqrt{g}\beta^{\lambda\mu_1..\mu_p}) = -D_\lambda\beta^{\lambda\mu_1\dots\mu_p}. \tag{5.11}$$

We can then define a Laplacian on p-forms by

$$\Delta = d\delta + \delta d. \tag{5.12}$$

The operators d, δ are nilpotent, i.e. $d^2 = \delta^2 = 0$, which implies that they commute with the Laplacian:

$$\begin{aligned} d\Delta &= \Delta d, \\ \delta\Delta &= \Delta\delta. \end{aligned} \tag{5.13}$$

Note that if on the LHS Δ acts on p-forms, then on the RHS it acts on $(p+1)$-forms or $(p-1)$-forms, respectively.

On scalar functions (zero-forms) is acts as the usual Laplacian or Laplace Beltrami operator: $\Delta f = -D^2 f$. On one-forms its action is given by

$$\Delta\omega_\mu = -D^2\omega_\mu + R_\mu{}^\nu\omega_\nu, \tag{5.14}$$

and one two-forms

$$\Delta\omega_{\mu\nu} = -D^2\omega_{\mu\nu} + R_\mu{}^\rho\omega_{\rho\nu} + R_\nu{}^\rho\omega_{\mu\rho} - 2R_\mu{}^\rho{}_\nu{}^\sigma\omega_{\rho\sigma}. \tag{5.15}$$

The Lichnerowicz Laplacians are the generalization of this construction. The action of the Lichnerowicz Laplacian on an arbitrary covariant p-tensor is defined by

$$(\Delta_{L_p} T)_{\mu_1..\mu_p} = -D^2 T_{\mu_1...\mu_p} + \sum_k R_{\mu_k}{}^{\rho} T_{\mu_1...\rho..\mu_p} - \sum_{k\neq l} R_{\mu_k}{}^{\rho}{}_{\mu_l}{}^{\sigma} T_{\mu_1...\rho...\sigma...\mu_p}. \tag{5.16}$$

The indices ρ and σ are in positions k and l respectively. Metric compatibility $D_\rho g_{\mu\nu} = 0$ then allows us to freely raise and lower indices, which gives us the definition of the Lichneworicz Laplacian on tensors of any rank. For example on symmetric 2-tensors it acts as

$$(\Delta_{L_2} T)_{\mu\nu} = -D^2 T_{\mu\nu} + R_\mu{}^\rho T_{\rho\nu} + R_\nu{}^\rho T_{\rho\mu} - 2R_\mu{}^\rho{}_\nu{}^\sigma T_{\rho\sigma}. \tag{5.17}$$

The Lichnerowicz Laplacian preserves the type and the symmetries of the tensor it acts on. It is self-adjoint and it commutes with contractions. It coincides with (5.12) when acting on totally antisymmetric tensors. On Einstein manifolds, i.e. if $R_{\mu\nu}$ is proportional to $g_{\mu\nu}$, it commutes with the covariant derivative. Therefore one has

$$\Delta_{L_1} D_\mu \phi = D_\mu \Delta_{L_0} \phi, \tag{5.18}$$
$$D_\mu \Delta_{L_1} \xi^\mu = \Delta_{L_0} D_\mu \xi^\mu, \tag{5.19}$$
$$\Delta_{L_2} g_{\mu\nu} \phi = g_{\mu\nu} \Delta_{L_0} \phi, \tag{5.20}$$

and other similar relations. In particular, (5.19) implies that if ξ^μ is a transverse vector (i.e. $D_\mu \xi^\mu = 0$), then $\Delta_{L_1} \xi^\mu$ is also transverse. For examples of uses of these Laplacians in the context of gravity we refer to the book [19].
In light of (5.16), we would define our endomorphism not only proportional to the Ricci scalar but also to contain the Riemann and Ricci tensors. However we project this information out by restricting the theory space to functions of only the scalar curvature. This is best seen when we employ a maximally symmetric background in (4.33); all contributions from Riemann and Ricci tensors turn into scalar curvature contributions. Due to the index structure of both (5.16) and (4.33), all metric terms becomes Kronecker deltas. In this sense our truncation is not sensitive to other curvature contributions.

5.3 Positive semi-definiteness and Equal Lowest Eigenvalue

One way to fix the values of α is to use the principle of equal lowest eigenvalues [28]. The goal of this principle is to adjust the values of α_s so that the lowest eigenvalue modes of different spin sectors are integrated out at the same value k_0. We can apply this to our calculation in chapter 4. Again assuming a spherical background, for fluctuation modes to be integrated out at the same k_0, the ratio[15] between the eigenvalue of $\Box$ and k_0^2 needs to be the same for both sectors. Applying this principle to the traceless tensors and scalars in chapter 4, for which we can read off the lowest eigenvalues in (4.64), entails to requiring

$$\frac{\frac{1}{6}R + \alpha_T R}{k_0^2} = \frac{\alpha_S R}{k_0^2}. \tag{5.21}$$

This straightforwardly implies the following relation between α_S and α_T on a spherical background:

$$\alpha_S = \alpha_T + \frac{1}{6}. \tag{5.22}$$

[15] A canonical choice for this ratio is 1, in particular with regulators with a sharp profile such as (5.4), as they reach 0 exactly at this point. This definition is also used with the exponential cutoff, which still has some suppression at this point. However, the value of this ratio does not matter for the equal lowest eigenvalue principle. Likewise, at which scale k_0 these modes are integrated out does not matter either. Choosing this scale fixes the remaining freedom of this principle.

The vector part with α_V can be included as well. In the end this will give 3 equations of which 2 are linearly independent, which means that the α_s are fixed when one of them is chosen. By construction this will adhere to the bounds (4.66), unless one of them is empty, because the lower bound is a trivial solution to (5.21). In fact, all intervals of good α_s values shrink in size to the size of the smallest interval. If one has a way of selecting the "right" coarse graining operator in one sector, this principle can be used to extend this choice to all other spin fields. This remaining freedom can be fixed by demanding that the lowest eigenmode is integrated out at $k_0 = 0$, which sets the numerators of (5.21) to zero[16] and fixes α_s to the lower bounds of (4.66). Since in chapter 4 the only admissible value for α_S was zero, this was already implicit and α_s are on their lowest possible values, i.e. $\alpha_T = -1/6$, $\alpha_S = 0$, $\alpha_V = -7/12$.

[16] Recall that the regulator scales as $R_k(0) \sim k^2$ and so the lowest eigenmode is indeed unsuppressed only at $k = 0$.

6 Relating regularization procedures in the exact case

In this chapter we will study the effects of changing the cutoff function R_k. Most of the techniques used are general enough to be applicable to all regulator changes, instead of specifically catering to a change of coarse graining operators. Therefore the analysis will start in the general case, and the result will be looked at in terms of this specific regulator change. There are two strategies we will work out in this chapter: in chapter 6.1 we makes use of a field transformation which maps the regulator terms to each other. This transformation is then carried through from the path integral to the effective average action in order to relate the two. In chapter 6.2 we use equation (2.30) and study the scale derivative of this deformation, in particular how the deformation commutes with respect to the scale derivative. In order to lighten our notation, we will suppress internal indices in this chapter.

6.1 Field transformation

In this section we will derive a map between the flows of effective average actions resulting from different regulators. To do so, we introduce regulators indexed by superscripts $R_k^{(1)}, R_k^{(2)}$. Although much of the analysis holds for general regulator change, we will think of the difference being in the coarse graining operator, i.e.

$$\begin{aligned} \Box^{(1)} &\equiv -\Delta, \\ \Box^{(2)} &\equiv -\Delta + \alpha \bar{R}, \quad \alpha \neq 0, \end{aligned} \tag{6.1}$$

with $\bar{R}$ the background curvature. Hence $R_k^{(1)}, R_k^{(2)}$ will indicate regulators that use their respective operators. Other functionals which contain these functions will also contain these superscripts. We will require the regulators to be invertible and to have a square root. The regulator terms in the modified path integral can be related by a $(k^2, p^2, \bar{R})$-dependent transformation of h:

$$\Delta_k S^{(2)}[h] = \frac{1}{2} \int d^d x \sqrt{g}\, h R_k^{(2)} h = \frac{1}{2} \int d^d x \sqrt{g}\, h \sqrt{\frac{R_k^{(2)}}{R_k^{(1)}}} R_k^{(1)} \sqrt{\frac{R_k^{(2)}}{R_k^{(1)}}} h = \Delta_k S^{(1)}[\widetilde{h}]. \tag{6.2}$$

$$\widetilde{h} \equiv \sqrt{\frac{R_k^{(2)}}{R_k^{(1)}}} h. \tag{6.3}$$

In general, this field transformation will be nonlocal, i.e. it contains arbitrarily high derivative terms. We can look at the basis decomposition of h and $\widetilde{h}$. Assuming the field can be decomposed in eigenfunctions T_n of Δ, this gives

$$h = \sum_n a_n T_n, \tag{6.4}$$

$$\widetilde{h} = \sum_n \widetilde{a}_n(p^2, k^2, \bar{R}) T_n. \tag{6.5}$$

The transformed basis coefficients $\widetilde{a}_n$ now have a p^2 dependence because of the momentum dependence of the regulators. We can apply the Laplacian in order to see what happens to its spectrum:

$$-\Delta h = \sum_n p_n^2 a_n T_n, \tag{6.6}$$

$$-\Delta \widetilde{h} = \sum_n p_n^2 \widetilde{a}_n(p^2, k^2, \bar{R}) T_n - \sum_n \Delta \widetilde{a}_n(p^2, k^2, \bar{R}) T_n. \tag{6.7}$$

Here p_n^2 indicate eigenvalues of the basis elements T_n. We can see that as long as the regulator only contains covariantly constant quantities, the transformation (6.3) will map momentum eigenmodes to momentum eigenmodes with the same eigenvalue, but will change expansion coefficients.
From this transformation it becomes clear why we need an invertible cutoff, such as the exponential cutoff (2.8). Since we divide by $R_k^{(1)}$, we can not have this be 0. Also if $R_k^{(2)}$ is 0 somewhere, then the transformation is not invertible. This causes problems in the following steps when we define a suitable dual variable (source) for the transformed field, as this will use the inverse transformation. Evaluating the $k \to 0$ limit for the exponential cutoff for the transformation gives $\sqrt{\frac{R_k^{(2)}}{R_k^{(1)}}} \to 0$ when α is positive, or $\sqrt{\frac{R_k^{(2)}}{R_k^{(1)}}} \to \infty$ when α is negative. Checking this limit for a change in parameter s parameterizing the family of exponential cutoffs (2.10), where $R_k^{(1)}$ uses the value $s = 1$ and $R_k^{(2)}$ uses a different s, gives the same qualitative behaviour around the point $s = 1$ in the sense that it diverges for $s < 1$ and goes to 0 for $s > 1$. This is a generic feature of this transformation: both $R_k^{(1)}$ and $R_k^{(2)}$ go to 0 in the limit $k \to 0$, and generally their asymptotic behaviour as a function of k will differ, which is to say one of them will approach zero quicker than the other. If $R_k^{(2)}$ has a steeper descent to 0, then the limit will go to 0 and if $R_k^{(1)}$ has a steeper descent then the limit will go to ∞. Only $R_k^{(1)} \propto R_k^{(2)}$ (where the proportionality constant can still contain momentum and curvature) as $k \to 0$ will result in a finite, nonzero limit which is necessary for invertibility. This shows that this transformation is only valid for $k > 0$. Because the regulator drops out at $k = 0$, which leads to both effective average actions being the same, we can exclude this point without any direct issues. However, one should keep this in mind if one analyzes the results of this chapter in the IR regime. In the UV limit this transformation will be finite because the regulators are required to diverge as k^2. In the case (6.1) the regulators diverge with the same proportionality constant and so in the UV limit this transformation maps h to itself, since $\sqrt{\frac{R_k^{(2)}}{R_k^{(1)}}} \to 1$ for $k \to \infty$. From here we will always assume h is k independent, while $\widetilde{h}$ is k dependent. With this we can relate the path integrals with different cutoff actions:

$$\begin{aligned} Z_k^{(2)}[J] &\equiv \int Dh e^{-S[h]} e^{Jh} e^{-\Delta_k S^{(2)}[h]} = \int Dh e^{-S[h]} e^{Jh} e^{-\Delta_k S^{(1)}[\widetilde{h}]} \\ &= \det\left(\sqrt{\frac{R_k^{(1)}}{R_k^{(2)}}}\right) \int D\widetilde{h} e^{-S[h]} e^{Jh} e^{-\Delta_k S^{(1)}[\widetilde{h}]}. \end{aligned} \tag{6.8}$$

In order to perform the integration, we can write h as function of $\widetilde{h}$ so that the action, source, and regulator terms have the same argument. This introduces a new (k-dependent!) bare action and source $\widetilde{S}, \widetilde{J}$, defined by

$$\widetilde{S}[\widetilde{h}] = S[h], \tag{6.9}$$

$$\widetilde{Jh} = Jh. \tag{6.10}$$

Explicitly, this means that $\widetilde{J} = \sqrt{\frac{R_k^{(1)}}{R_k^{(2)}}} J$, necessitating that the field transformation is invertible. Note that, while $\widetilde{S}$ and $\widetilde{J}$ are k-dependent, their k-dependence is exactly such that $\widetilde{S}[\widetilde{h}]$ and $\widetilde{Jh}$ are k-independent. Furthermore, the equations of motion retain their form with this transformation, i.e. $\delta S[h]/\delta h = J$ if and only if $\delta \widetilde{S}[\widetilde{h}]/\delta \widetilde{h} = \widetilde{J}$. These new scale dependent functionals will be used to construct an Effective Average Action, as such, this EAA will inherit this tilde notation in a similar way to $\widetilde{S}$. Using this we continue our computation of Z_k:

$$Z_k^{(2)}[J] = \det\left(\sqrt{\frac{R_k^{(1)}}{R_k^{(2)}}}\right) \int D\widetilde{h} e^{-\widetilde{S}[\widetilde{h}]} e^{\widetilde{Jh}} e^{-\Delta_k S^{(1)}[\widetilde{h}]} = \det\left(\sqrt{\frac{R_k^{(1)}}{R_k^{(2)}}}\right) \widetilde{Z}_k^{(1)}[\widetilde{J}]. \tag{6.11}$$

Here we have defined the functional $\widetilde{Z}_k^{(1)}[\widetilde{J}]$ by

$$\widetilde{Z}_k^{(1)}[\widetilde{J}] \equiv \int D\widetilde{h} e^{-\widetilde{S}[\widetilde{h}]} e^{\widetilde{J}\widetilde{h}} e^{-\Delta_k S^{(1)}[\widetilde{h}]}. \tag{6.12}$$

Here the tilde on the functional Z_k itself indicates the transform of the bare action functional (6.9) and the tilde on the source argument indicates the transformation (6.10) has been done. The EAA we will arrive at later will have the same tilde notation structure. The determinant is field and source independent and cancels if the path integral is normalized. We will discuss its contribution later on but for now we will discard this factor and introduce the Schwinger functionals, defined with the same convention as the path integrals:

$$W_k^{(2)}[J] \equiv \log[Z^{(2)}[J]], \tag{6.13}$$

$$\widetilde{W}_k^{(1)}[\widetilde{J}] \equiv \log[\widetilde{Z}^{(1)}[\widetilde{J}]]. \tag{6.14}$$

Neglecting the determinant (which vanishes if we normalize) we straightforwardly find

$$W_k^{(2)}[J] = \widetilde{W}_k^{(1)}[\widetilde{J}]. \tag{6.15}$$

To get a relation between the effective average actions, we will need to see how the field expectation values are related. The relevant field expectation values are defined as

$$\chi^{(2)} \equiv \langle h \rangle_{S,J} = \frac{\delta W_k^{(2)}}{\delta J}, \tag{6.16}$$

$$\hat{\chi}^{(1)} \equiv \langle \widetilde{h} \rangle_{\widetilde{S},\widetilde{J}} = \frac{\delta \widetilde{W}_k^{(1)}}{\delta \widetilde{J}} = \frac{\delta J}{\delta \widetilde{J}} \frac{\delta W_k^{(2)}}{\delta J} = \sqrt{\frac{R_k^{(2)}}{R_k^{(1)}}} \chi^{(2)}. \tag{6.17}$$

One should keep in mind that $\hat{\chi}^{(1)}$ is quantized from the scale-dependent system $(\widetilde{S}, \widetilde{J})$, evident from the subscripts. This computation implies that the field expectation values have the same transformation as the quantum fields in (6.3), i.e.

$$\hat{\chi}^{(1)} = \sqrt{\frac{R_k^{(2)}}{R_k^{(1)}}} \chi^{(2)} \equiv \widetilde{\chi^{(2)}}. \tag{6.18}$$

Similar relations with the appropriate power of the transformation $(\frac{R_k^{(2)}}{R_k^{(1)}})^{n/2}$ hold for n-point functions, e.g. $\langle \widetilde{h}\widetilde{h} \rangle_{\widetilde{S},\widetilde{J}} = \frac{R_k^{(2)}}{R_k^{(1)}} \langle hh \rangle_{S,J}$ for the two point function. Since if we disregard the cutoff action the relation (6.11) can be made for any field transformations. The same method can be used in general for field transformations in path integrals at $k = 0$. With these results we can construct the effective average actions

$$\Gamma_k^{(2)}[\chi^{(2)}] \equiv \sup_J \left[J\chi^{(2)} - W_k^{(2)}[J] \right] - \Delta_k S^{(2)}[\chi^{(2)}], \tag{6.19}$$

$$\widetilde{\Gamma}_k^{(1)}[\hat{\chi}^{(1)}] \equiv \sup_{\widetilde{J}} \left[\widetilde{J}\hat{\chi}^{(1)} - \widetilde{W}_k^{(1)}[\widetilde{J}] \right] - \Delta_k S^{(1)}[\hat{\chi}^{(1)}]. \tag{6.20}$$

The tilde on $\widetilde{\Gamma}_k^{(1)}$ is there to represent that it is quantized from the scale-dependent bare action. Using (6.10), (6.15), and (6.18) we can easily see that these two expressions are equal. So we come to the main conclusion of this chapter, easing notation and interpreting χ as some k independent field and $\widetilde{\chi}$ its transformation by (6.3), we conclude:

$$\boxed{\Gamma_k^{(2)}[\chi] = \widetilde{\Gamma}_k^{(1)}[\widetilde{\chi}]}. \tag{6.21}$$

So the field transformation (6.3) has the desired and expected result at the level of the effective average action as well. Note that, if we express the RHS in terms of the k independent basis of functionals of χ, we will introduce factors $\sqrt{\frac{R_k^{(2)}}{R_k^{(1)}}}$. These can be expanded in a Taylor series in both momentum and curvature which results in higher order kinetic and curvature terms[17]. In the example in chapter 5, the first term to be generated by this expansion which is not included in the truncation is $\bar{R}\bar{\psi}\psi$. This equation also reaffirms the idea that changing the regulator amounts to a basis transformation in theory space. Including the determinant prefactor we discarded earlier leads to an extra term in the equation of the form $\mathrm{Tr}\ln\left(\sqrt{\frac{R_k^{(1)}}{R_k^{(2)}}}\right)$. This contribution is generally ill-defined as it contains infinities. The fraction of the two regulators no longer has the falloff properties necessary for the integrals resulting from the trace to be finite. We shall show this in the case of coarse graining operators described by (6.1), up to first order in the endomorphism parameter α and background curvature $\bar{R}$. Expanding the regulator $R_k^{(2)}$ around $\alpha = 0$, the contribution is then

$$\mathrm{Tr}\left[\frac{\alpha\bar{R}}{k^2}\frac{R_k^{(1)\prime}}{R_k^{(1)}}\right] + \mathcal{O}((\alpha\bar{R})^2) \sim \frac{\alpha\bar{R}}{k^2}\int_0^\infty dz\, z\frac{R'(z)}{R(z)} + \mathcal{O}(\alpha^2, \bar{R}^2). \tag{6.22}$$

Here constant factors appearing in heat kernel calculations are discarded as they are not relevant to the discussion. On the LHS the higher order terms are in terms of the product $\alpha\bar{R}$, while on the RHS these split because of the heat kernel expansion. The integration is over the variable $z = \frac{p^2}{k^2}$, and on the RHS we have renamed $R_k^{(1)}(z) \to R(z)$. Substituting the exponential cutoff (2.9), the expression reads

$$\frac{\alpha\bar{R}}{k^2}\int_0^\infty dz\, z\frac{R'(z)}{R(z)} = \frac{\alpha\bar{R}}{k^2}\int_0^\infty dz\frac{1+e^z(z-1)}{1-e^z}. \tag{6.23}$$

The integral can be solved in closed form, but we can already see from the integrand that this will diverge at the upper boundary. Evidently, the proper falloff behaviour does not hold for the fraction of regulators. Similar effects happen for other choices of shape functions and higher order terms. This justifies neglecting this term as we did earlier, which has the interpretation of normalizing the path integral such that the determinant cancels.

Having quantized $\widetilde{\Gamma}_k^{(1)}[\widetilde{\chi}]$ from a scale dependent bare action should not matter for its UV limit(in the exact case), since we have (2.29) and $\sqrt{\frac{R_k^{(2)}}{R_k^{(1)}}} \to 1$ for $k \to \infty$, which implies $\widetilde{\Gamma}_k \to \widetilde{S} \to S$ for $k \to \infty$. This is in line with the fact that the fixed point is independent of the regulator. Furthermore, in a practical calculation one would find the consistent theories for the effective average action and construct the bare action from that, meaning that as long as (2.29) holds, the correct bare action is found. However, in a truncation this relation does not precisely hold, resulting in a fixed point which depends on the choice of regulator.
Coming back to the issue the field transformation (6.3) has in the $k \to 0$ limit, we note that there is seemingly a mismatch between the IR limit of (6.21) and the IR limit of the definition of the Effective Average Action (2.13). In the definition of the EAA the regulator effects vanish when $k \to 0$ as long as the general prerequisites are met, regardless of any specifics of the regulator. However, from the view of RG flows, when following the RG flow down from the (vicinity of) the fixed point, it is not surprising that a different regulator implies a different endpoint of the flow.
We can write down (6.21) in component form. Consider for example a scalar field theory with a single scalar field ϕ. Consistently including the wavefunction renormalization constant z_k with appropriate power in each term, one can apply a transformation on the wavefunction renormalization instead of the field. Redefining the field to incorporate this $\phi \to z_k^{1/2}\phi$ we have the freedom to let the field transformation defined by (6.3)

[17] Equivalently, one can absorb these series in the couplings and examine momentum or curvature dependent couplings.

work only on z_k instead, i.e.:

$$\widetilde{\phi} = \phi, \tag{6.24}$$

$$\widetilde{z_k} = \frac{R_k^{(2)}}{R_k^{(1)}} z_k. \tag{6.25}$$

Here $z_k \equiv z_k^{(2)}$ is a coupling of the EAA $\Gamma_k^{(2)}$ and $\widetilde{z_k}$ appears in $\widetilde{\Gamma}_k^{(1)}$. The z_k must depend on momentum and possibly the curvature, going beyond being just a wavefunction renormalization. The advantage of this is that it can compensate regulator effects with one coupling constant, in the sense that the regulator terms can be factorized and absorbed into z_k. This provides a very direct test of how well this method based on the field transformation (6.3) achieves its desired result in a truncation. Because of the earlier IR features we commented on earlier, the coupling is not well-behaved in the IR. In particular, the anomalous dimension $\widetilde{\eta}- \equiv \partial_t \ln(\widetilde{z}_k)$ receives a contribution

$$\widetilde{\eta} = \eta - \partial_t \ln\left(\frac{R_k^{(2)}}{R_k^{(1)}}\right) \equiv \eta + \delta\eta, \tag{6.26}$$

which is divergent for $k \to 0$ for both positive and negative α.

6.1.1 In the background field formalism

In preparation for the application to the Einstein-Hilbert truncation later on, we will examine the previous result using the background field formalism. Recall that in this method, only the fluctuation field is suppressed by the cutoff action. Therefore the field transformation (6.3) only works on the fluctuation field and the final result (6.21) in terms of the fluctuation field h and background field $\bar{g}$ reads

$$\Gamma_k^{(2)}[h;\bar{g}] = \widetilde{\Gamma}_k^{(1)}[\widetilde{h};\bar{g}]. \tag{6.27}$$

In single-metric calculations the fluctuation fields are set to 0 after taking variations on the RHS. Thus the flow will be affected and so this equation itself is not directly helpful. It is then useful to compute the the resulting change in the flow. When doing this we need to keep in mind that the derivation of the FRGE assumes the field and RG scale as independent variables. This independence is manifestly broken by our field transformation. In tensor language, we can then define two coordinate systems:

$$\begin{aligned} &R_k^{(2)} \text{ system}: \ x^\mu = (h,t) && \partial_t h = 0 \\ &R_k^{(1)} \text{ system}: \ \widetilde{x}^\mu = (\widetilde{h},\widetilde{t}) && \widetilde{h} \equiv \sqrt{\frac{R_k^{(2)}}{R_k^{(1)}}} h, \quad \widetilde{t} = t \end{aligned} \tag{6.28}$$

Even though we have $\widetilde{t} = t$, their differentials are different. Using the familiar language of coordinate transforms with tensors, we find

$$\partial_{\widetilde{t}}\Gamma_k = \partial_t\Gamma_k - \frac{\delta\Gamma_k}{\delta h}\frac{\partial h}{\partial \widetilde{h}}\frac{\partial \widetilde{h}}{\partial t} = \partial_t\Gamma_k - \frac{\delta\Gamma_k}{\delta h}\sqrt{\frac{R_k^{(1)}}{R_k^{(2)}}}\partial_t\sqrt{\frac{R_k^{(2)}}{R_k^{(1)}}}h \equiv \partial_t\Gamma_k + \frac{\delta\Gamma_k}{\delta h}\eta_{\mathcal{A}} h. \tag{6.29}$$

$$\eta_{\mathcal{A}} \equiv -\frac{1}{2}\partial_t \log[\frac{R_k^{(2)}}{R_k^{(1)}}] \tag{6.30}$$

Here we have defined $\eta_{\mathcal{A}}$, which can be interpreted as the anomalous dimension of the transformation. In the last term[18] we omitted the integral over spacetime and contraction over internal indices. The contribution originating from the coordinate transform is proportional to the effective equations of motion, and linear in the fluctuation field. Because of the former, this does not contribute to on-shell calculations at $k = 0$. Because of the latter, it does not contribute at all in the single-metric approximation. By construction of the system (6.28) we have $\partial_{\widetilde{t}}\widetilde{h} = 0$, which means that $\partial_{\widetilde{t}}\widetilde{\Gamma}_k^{(1)}[\widetilde{h};\bar{g}]$ obeys a Wetterich equation. Writing it out we derive

$$\begin{aligned}
\partial_{\widetilde{t}}\widetilde{\Gamma}_k^{(1)}[\widetilde{h};\bar{g}] &= \frac{1}{2}\,\mathrm{Tr}\left[(\frac{\delta^2\widetilde{\Gamma}_k^{(1)}}{\delta\widetilde{h}\delta\widetilde{h}} + R_k^{(1)})^{-1}\partial_t R_k^{(1)}\right] \\
&= \frac{1}{2}\,\mathrm{Tr}\left[(\frac{\delta^2\Gamma_k^{(2)}}{\delta h\delta h} + R_k^{(2)})^{-1}\frac{R_k^{(2)}}{R_k^{(1)}}\partial_t R_k^{(1)}\right] \\
&= \frac{1}{2}\,\mathrm{Tr}\left[(\frac{\delta^2\Gamma_k^{(2)}}{\delta h\delta h} + R_k^{(2)})^{-1}(\partial_t R_k^{(2)} - R_k^{(2)}\partial_t\log[\frac{R_k^{(2)}}{R_k^{(1)}}])\right] \\
&= \partial_t\Gamma_k^{(2)}[h;\bar{g}] + \mathrm{Tr}\left[(\frac{\delta^2\Gamma_k^{(2)}}{\delta h\delta h} + R_k^{(2)})^{-1}R_k^{(2)}\eta_{\mathcal{A}}\right].
\end{aligned} \tag{6.31}$$

The change in superscript of the Hessian in the second equality is allowed precisely because of (6.27). The anomalous dimension $\eta_{\mathcal{A}}$ appears again in this equation, giving an indication of the magnitude of the extra contributions. Combining this with the previous relation, we find

$$\partial_t\widetilde{\Gamma}_k^{(1)}[\widetilde{h};\bar{g}] = \partial_t\Gamma_k^{(2)}[h;\bar{g}] + \mathrm{Tr}\left[(\frac{\delta^2\Gamma_k^{(2)}}{\delta h\delta h} + R_k^{(2)})^{-1}R_k^{(2)}\eta_{\mathcal{A}}\right] - \frac{\delta\Gamma_k^{(2)}}{\delta h}\eta_{\mathcal{A}}h. \tag{6.32}$$

This relation encodes the difference of two RG flows when the regulator has changed, but no redefinition of the RG scale k has been done. The last term has been written in terms of $\Gamma_k^{(2)}$ once again using (6.21). Note that in this equation h and t are independent variables, assuming $\widetilde{h}$ and t to be independent (i.e. expressing the equation in $\partial_{\widetilde{t}}$) changes the sign of the last term.
Furthermore, as the field transformation works only on the fluctuation field, the split symmetry also transforms in a complex way, since the field transformation depends on $\bar{g}$ in a very nontrivial way because of the different $\bar{g}$-dependence of $R_k^{(1)}$ and $R_k^{(2)}$. The modified Ward Identity (4.20) will also be deformed by the transformation.

6.2 Deformation of the Effective Average Action

We can use the Wetterich equation to study the effect of a change in the coarse graining operator $\Box$. Writing down the equation for a coarse graining operator $\Box = -\Delta$, we can deform this by introducing a infinitesimal α in $\Box$. We can compare this to the flow of the deformation to the effective average action, essentially checking the commutation of taking the flow (∂_t) and deforming the regulator (δR_k). We recall the FRGE and the deformation of the EAA by a deformed regulator

$$\delta\Gamma_k = \frac{1}{2}\mathrm{Tr}\left[\left(\Gamma_k'' + R_k\right)^{-1}\delta R_k\right], \tag{6.33}$$

$$\partial_t\Gamma_k = \frac{1}{2}\mathrm{Tr}\left[\left(\Gamma_k'' + R_k\right)^{-1}\partial_t R_k\right]. \tag{6.34}$$

[18] A more general version of this term was also found in [29] in the context of bosonization. The general version appears generically due to scale dependent fields.

To ease the notation we have written down the Hessian as $\Gamma_k'' \equiv \frac{\delta^2\Gamma_k}{\delta h \delta h}$. The infinitesimal deformation of regulator δR_k in terms of the endomorphism parameter α has the following form at linear order in α,

$$\delta R_k = \alpha \bar{R} R_k', \tag{6.35}$$

where the prime indicates a derivative with respect to its (here dimensionful) argument. Starting from the FRGE (6.34), an infinitesimal transformation of the regulator, $R_k \to R_k + \delta R_k$, yields the following expression for the deformation of the flow

$$\delta\partial_t\Gamma_k = \frac{1}{2}\mathrm{Tr}\left[\left(\Gamma_k'' + R_k\right)^{-1}\delta\partial_t R_k - \left(\Gamma_k'' + R_k\right)^{-1}\left(\delta\Gamma_k'' + \delta R_k\right)\left(\Gamma_k'' + R_k\right)^{-1}\partial_t R_k\right). \tag{6.36}$$

Likewise, we can first deform the regulator, and then compute the flow of this effect. Now starting from the deformation (6.33), the infinitesimal transformation evolves as

$$\partial_t\delta\Gamma_k = \frac{1}{2}\mathrm{Tr}\left[\left(\Gamma_k'' + R_k\right)^{-1}\partial_t\delta R_k - \left(\Gamma_k'' + R_k\right)^{-1}\left(\partial_t\Gamma_k'' + \partial_t R_k\right)\left(\Gamma_k'' + R_k\right)^{-1}\delta R_k\right). \tag{6.37}$$

We can now compare these two expressions. In fact, we will calculate their difference, which amounts to computing the effect of the commutator $[\delta, \partial_t]$ on Γ_k. Assuming that the regulator is a C^2 function we have that $\partial_t\delta R_k = \delta\partial_t R_k$, and thus the first term cancels. The remaining terms then give

$$\begin{aligned}[\delta, \partial_t]\Gamma_k = -\frac{1}{2}\,\mathrm{Tr}\Big[\left(\Gamma_k'' + R_k\right)^{-1}\Big(&(\partial_t\Gamma_k'' + \partial_t R_k)(\Gamma_k'' + R_k)^{-1}\delta R_k \\ &- \left(\delta\Gamma_k'' + \delta R_k\right)\left(\Gamma_k'' + R_k\right)^{-1}\partial_t R_k\Big)\Big].\end{aligned} \tag{6.38}$$

The terms $(\Gamma_k'' + R_k)^{-1}\partial_t R_k(\Gamma_k'' + R_k)^{-1}\delta R_k$ and $(\Gamma_k'' + R_k)^{-1}\delta R_k(\Gamma_k'' + R_k)^{-1}\partial_t R_k$ cancel against each other due to the cyclic property of the trace. For the other terms we note the commutation relations $[\frac{\delta}{\delta h}, \partial_t]\Gamma_k = 0 = [\frac{\delta}{\delta h}, \delta]\Gamma_k$, which hold because δ and ∂_t work on the couplings while $\frac{\delta}{\delta h}$ works on the fields. We can then commute the field derivative with the scale derivative or regulator deformation i.e. $\partial_t\Gamma_k'' = (\frac{\delta^2}{\delta h\delta h})\partial_t\Gamma_k$, and use the equations (2.14), (2.30) for the $\partial_t\Gamma_k''$ and $\delta\Gamma_k''$ terms. This substitution results in

$$\begin{aligned}[\delta, \partial_t]\Gamma_k = -\frac{1}{2}\,\mathrm{Tr}\Big[(\Gamma_k'' + R_k)^{-1}\Big(&(\frac{\delta^2}{\delta h\delta h}\,\mathrm{Tr}\left\{(\Gamma_k'' + R_k)^{-1}\partial_t R_k\right\})(\Gamma_k'' + R_k)^{-1}\delta R_k \\ &- (\frac{\delta^2}{\delta h\delta h}\,\mathrm{Tr}\left\{(\Gamma_k'' + R_k)^{-1}\delta R_k\right\})(\Gamma_k'' + R_k)^{-1}\partial_t R_k\Big)\Big].\end{aligned} \tag{6.39}$$

Rather than going into the full index structure and momentum integration, it is intuitive to look at this equation in a diagrammatic picture. Here $(\Gamma_k'' + R_k)^{-1}$ is the full propagator and so is indicated with a line, and functional derivatives $\frac{\delta}{\delta h}$ create a vertex by adding an external line to the object it acts on. Because the entire expression is inside a trace there are no external lines and thus all lines are contracted. Furthermore, higher derivates of the EAA $\Gamma_k^{(n)}$ are by construction the n-point functions or the effective n-vertices. We recall the wetterich equation in this diagrammatic notation:

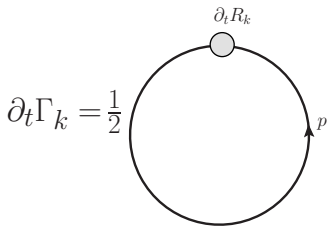

Figure 4: The Wetterich equation in diagrammatic form which has a one-loop structure. The momentum p in the loop is integrated over. The grey blob with $\partial_t R_k$ indicates that this loop is regulated by a factor $\partial_t R_k$.

The grey blob indicates that the loop is regulated by a factor $\partial_t R_k$. The innermost trace in (6.39) has the same structure because of the substitution of the FRGE and (2.30). Because two field derivatives work on it, it gains two external legs, which are contracted with the other propagators in the trace. This leads to a diagram with two 3-point vertices and a diagram with one 4-point vertex. The following diagrams are then generated by (6.39):

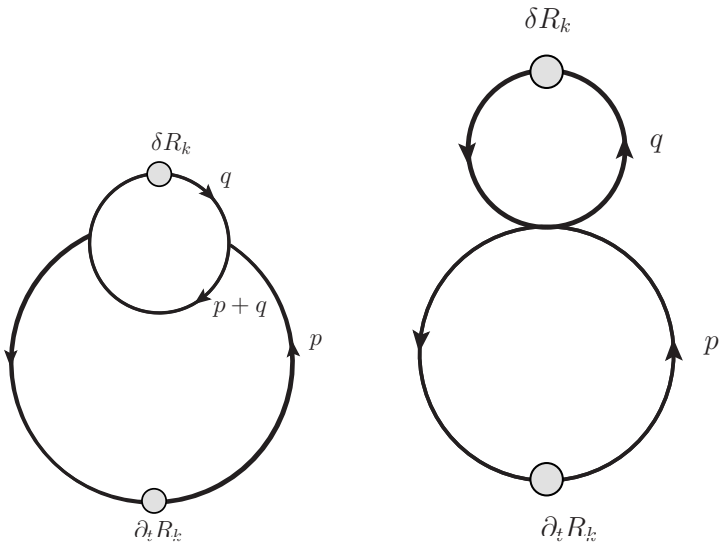

Figure 5: The diagrams corresponding to the commutation relation (6.39). Momentum flow is along the arrows and the grey blobs indicate regularization factors.

The commutation (6.39) is antisymmetric in swapping δR_k and $\partial_t R_k$, so the same diagrams with $p \leftrightarrow q$ occur with a minus sign. However, the diagrams of this expression are symmetric in the replacement $p \leftrightarrow q$, or in swapping δR_k and $\partial_t R_k$. Therefore the sum of all diagrams of (6.39) is zero:

$$[\delta, \partial_t]\Gamma_k = 0. \tag{6.40}$$

Note that the specific deformation (6.35) has not been used, meaning that it holds for any infinitesimal regulator deformation. Furthermore, it holds for all scales k. In particular the fixed point condition is unaffected by a deformation of the regulator.

7 Application to Einstein-Hilbert truncation

We have derived some exact results regarding a change of the coarse graining operator in chapter 6, and done a benchmark calculation in chapter 4. We can now compare these new exact results to our benchmark at the level of the corresponding truncation. We will use (2.30) to construct an RG flow for $\alpha \neq 0$ from the RG flow with $\alpha = 0$, and compare the extra terms to the flow equations from chapter 4 and the exact conclusion in chapter 6. Furthermore we will construct the extra terms in (6.32) in order to retrieve the $\alpha = 0$ case from a general α. In both these methods we will look at similarities in the beta functions and the effect on fixed point coordinates and critical exponents. We will apply a similar approximation for both methods, which is because of our choice of regulator (4.36), (4.37). The prefactor $\mathcal{Z}_k$ contains the coupling Z_k, which will be different for the regulators $R_k^{(1)}, R_k^{(2)}$ because of the different coarse graining operators. This difference of Z_k in front of the shape function will be neglected; with the field transformation this difference can be incorporated in the beta functions, but when working with the deformed EAA this requires a closed form for the coupling as a function of the scale k.

7.1 Application of the field transformation (FT)

We will now construct the extra terms occurring in (6.32) in the same Einstein-Hilbert setting. What should be achieved is that these extra terms (approximately) cancel the α-dependence found in the benchmark calculation. In particular, we would expect that the fixed point coordinates will be relatively stable around the $\alpha = 0$ case where they are given by $(\lambda_*, g_*) = (0.3590, 0.2723)$. As stated before, the term originating from the transformation of the differential ∂_t does not contribute in the single-metric approximation, so we are left with the equation

$$\partial_t \widetilde{\Gamma}_k^{(1)}[\widetilde{h};\bar{g}] = \partial_t \Gamma_k^{(2)}[h;\bar{g}] + \mathrm{Tr}\left[(\frac{\delta^2\Gamma_k^{(2)}}{\delta h \delta h} + R_k^{(2)})^{-1} R_k^{(2)} \eta_{\mathcal{A}}\right]. \tag{7.1}$$

First of all, because our truncation only goes up to first order in R, and $\eta_{\mathcal{A}} \equiv -\partial_t \log[\sqrt{\frac{R_k^{(2)}}{R_k^{(1)}}}] = 0 + \mathcal{O}(R)$, we are justified in neglecting all αR dependence of the second term that is not in $\eta_{\mathcal{A}}$, i.e. we can make the replacement $R_k^{(2)} \to R_k^{(1)}$. Also note that, similarly to before, we have different contributions for tensor fields, scalar fields, and the vector ghost fields. Using the same heat kernel methods and Hessian as before, the trace evaluates to

$$\frac{1}{(4\pi)^2}\,\mathrm{tr}_s[I]k^2 \int_0^\infty dz\; z\; \frac{R^{(0)}(z)\;\eta_{\mathcal{A}}}{z + R^{(0)}(z) + \omega} \int d^4x\sqrt{g} + \mathcal{O}(R^2) \tag{7.2}$$

Here the variable z does not contain the α : $z = -\frac{D^2}{k^2}$. The ω here takes on the values $-2\lambda_k$ for the tensor/scalar and zero for the vector parts respectively, and the vector part has an extra prefactor -2. An important remark to make is about an approximation we will employ: earlier in (4.36) we have the coupling Z_k included in the regulator function. Because of the α dependence of the flow equation, the prefactor Z_k will be different for $R_k^{(1)}, R_k^{(2)}$, resulting in a term proportional to $\delta\eta \equiv \eta^{(2)} - \eta^{(1)}$. A possibility is to substitute (4.56) with nonzero α values for the $\eta^{(2)}$ appearing in this expression, and solve the implicit equation for $\eta^{(1)}$. However, because a similar contribution for the deformed EAA does not have a closed form, we choose to not include this contribution.

To calculate this heat kernel integral we will need to choose the regulator. Inserting the exponential cutoff (2.8) or its shape function (2.9), the numerator of the new contribution reads, up to first order in the curvature:

$$zR^{(0)}\eta_{\mathcal{A}} \simeq \frac{z\left(e^z\left(z^2+2\right) - e^{2z} - 1\right)}{\left(e^z - 1\right)^3}\alpha R \tag{7.3}$$

One can verify that this can be expressed in the shape functions as

$$zR^{(0)}\eta_{\mathcal{A}} = \alpha R\left[-(R^{(0)}(z) - zR^{(0)\prime}(z)) + R^{(0)}(z)(R^{(0)}(z) - zR^{(0)\prime}(z)) - zR^{(0)\prime}(z)\right] + \mathcal{O}(R^2), \tag{7.4}$$

which is an identity that specifically holds for the exponential cutoff. We have ordered terms such that the correct combination for a Φ_1^1 threshold function appears. Since the new contributions are already first order in the Ricci scalar, the flow of the combination $(Z_k\Lambda_k)$ has no α dependence, as in the previous calculation. Aside from the Φ_1^1 threshold function, (7.4) also introduces terms which seemingly cannot be expressed in our regular threshold functions. We define new threshold functions for these terms:

$$\widehat{\Phi}_n^p(\omega) \equiv \frac{1}{\Gamma(n)}\int_0^\infty dz\; z^{n-1}\frac{R^{(0)}(z)^2 - zR^{(0)}(z)R^{(0)\prime}(z) - zR^{(0)\prime}(z)}{(z + R^{(0)}(z) + \omega)^p}. \tag{7.5}$$

Gathering (7.2), (7.4) and (7.5), we then conclude:

$$\begin{aligned}\mathrm{Tr}\left[(\frac{\delta^2\Gamma_k^{(2)}}{\delta h\delta h} + R_k^{(2)})^{-1}R_k^{(2)}\eta_{\mathcal{A}}\right] = \frac{1}{(4\pi)^2}\int d^4x\sqrt{g}Rk^2\Big[&-(9\alpha_T + \alpha_S)\big(\Phi_1^1(-2\lambda_k) - \widehat{\Phi}_1^1(-2\lambda_k)\big)\\ &+ 8\alpha_V\big(\Phi_1^1(0) - \widehat{\Phi}_1^1(0)\big)\Big]\end{aligned} \tag{7.6}$$

Comparing to (4.51) it is found that the additional term gives the same α dependence proportional with the Φ_1^1 functions occurring in (4.51), and also a new contribution from $\widehat{\Phi}_1^1$. The flow equations in terms of Λ_k and Z_k resulting from (7.1) then read

$$\partial_t(\Lambda_k Z_k)^{(1)} = \partial_t(\Lambda_k Z_k)^{(2)} = (4\kappa^2)^{-1}(4\pi)^{-2}k^4\Big[10\Phi_2^1(-2\lambda_k) - 8\Phi_2^1(0) - 5\eta\tilde{\Phi}_2^1(-2\lambda_k)\Big], \tag{7.7}$$

$$\begin{aligned}\partial_t Z_k^{(1)} = -(24\kappa^2)^{-1}(4\pi)^{-2}k^2\Big[&20(\Phi_1^1(-2\lambda_k) - \frac{1}{2}\eta\tilde{\Phi}_1^1(-2\lambda_k))\\ &- (108\alpha_T + 12\alpha_S)(2\Phi_1^1(-2\lambda_k) - \widehat{\Phi}_1^1(-2\lambda_k) - \frac{1}{2}\eta\tilde{\Phi}_1^1(-2\lambda_k))\\ &- (72 - 108\alpha_T - 12\alpha_S)\left(\Phi_2^2(-2\lambda_k) - \frac{1}{2}\eta\tilde{\Phi}_2^2(-2\lambda_k)\right)\\ &- 16\Phi_1^1(0) + 96\alpha_V(2\Phi_1^1(0) - \widehat{\Phi}_1^1(0)) - (24 + 96\alpha_V)\Phi_2^2(0)\Big].\end{aligned} \tag{7.8}$$

These equations are similar to before, with the only difference being the replacement $\Phi_1^1 \to 2\Phi_1^1 - \widehat{\Phi}_1^1$ where they appear with an α. Following the steps (4.52) to (4.54) results in the same form for the beta functions, where only the anomalous dimension η differs, i.e.

$$\eta(g_k, \lambda_k) = \frac{g_k B_1^{\mathrm{FT}}(\lambda_k, \alpha_s)}{1 - g_k B_2^{\mathrm{FRGE}}(\lambda_k, \alpha_s)}, \tag{7.9}$$

with B_1^{FT}

$$\begin{aligned}B_1^{\mathrm{FT}}(\lambda_k, \alpha_s) = B_1^{\mathrm{FRGE}}(\lambda_k, \alpha_s) + \frac{1}{3}(4\pi)^{-1}\Big[&-(108\alpha_T + 12\alpha_S)(\Phi_1^1(-2\lambda_k) - \widehat{\Phi}_1^1(-2\lambda_k))\\ &+ 96\alpha_V(\Phi_1^1(0) - \widehat{\Phi}_1^1(0))\Big]\end{aligned} \tag{7.10}$$

The superscript FT in B_1^{FT} stands for field transformation, to indicate how this was calculated. The function B_2 being unaffected is a direct result of our choice earlier in neglecting the difference in Z_k's or η's appearing in $\eta_{\mathcal{A}}$. Because of this, no extra η terms appear and the denominator in (4.56) and (7.10) are equal. All extra terms are proportional to the difference $\Phi_1^1 - \widehat{\Phi}_1^1$. This modification to the beta functions does not

appear to cancel the α dependence, which is what we would expect from a type I coarse graining. We shall look at the behaviour of the fixed point coordinates at the end of this chapter.

7.2 Application: deformation of the Effective Average Action (δR_K)

We will now look into the deformation of the Effective Average Action as described by (2.30), up to linear order in the Ricci scalar. In this context, the regulator has a coarse graining operator with $\alpha_s = 0$ and δR_k changes it into a regulator with a coarse graining operator with $\alpha_s \neq 0$. This entails to substituting (6.35) with nonzero α_s and the inverse propagators (4.38) with $\alpha_s = 0$. This results in

$$\delta\Gamma_k[g,g] = \mathrm{Tr}_T[\mathcal{B}_T(\mathcal{P} + \frac{2}{3}R)^{-1}] + \mathrm{Tr}_S[\mathcal{B}_S(\mathcal{P})^{-1}] - 2\,\mathrm{Tr}_V[\mathcal{B}_V(\mathcal{P}^{(0)} - \frac{1}{4}R)^{-1}]. \tag{7.11}$$

Here the $\mathcal{P}$ operators without subscript are the same as in (4.40), but with all α_s set to 0, and $\mathcal{B}_s$ plays the same role as $\mathcal{N}_s$, but for δR_k rather than $\partial_t R_k$. Explicitly, they read

$$\begin{aligned} \mathcal{P} &\equiv -D^2 + k^2 R^{(0)}(\frac{-D^2}{k^2}) - 2\Lambda_k, \\ \mathcal{B}_s &\equiv \frac{1}{2}k^2\alpha_s R R^{(0)\prime}(\frac{-D^2}{k^2}). \end{aligned} \tag{7.12}$$

We have made the same approximation here in writing the expression for $\mathcal{B}_s$ as we have in the last chapter: the extra term proportional $\frac{\delta Z_k}{Z_k^{(1)}}$ has been neglected, so we assume again that the Z_k appearing here does not change. Taking this term into account would require an explicit expression for $Z_k^{(1)}$, which we do not have without introducing initial conditions and integrating (4.51). This is unlike the previous method, where the term we left out can be included since we have an explicit equation for η. Since the $\mathcal{B}$ operators are linear in the curvature, expanding in powers of R is trivial:

$$\delta\Gamma_k[g,g] = \mathrm{Tr}_T[\mathcal{B}_T\mathcal{P}^{-1}] + \mathrm{Tr}_S[\mathcal{B}_S\mathcal{P}^{-1}] - 2\,\mathrm{Tr}_V[\mathcal{B}_V\mathcal{P}^{(0)\,-1}]. \tag{7.13}$$

Denoting $\mathcal{T}_s = \mathrm{Tr}_s[\mathcal{B}_s\mathcal{P}^{-1}]$, each of these traces is calculated by applying the heat kernel

$$\begin{aligned} \mathcal{T}_s &= \alpha_s\frac{1}{2}\frac{1}{(4\pi)^2}\,\mathrm{tr}_s[I]k^2\int_0^\infty dz\;\frac{zR^{(0)\prime}(z)}{z + R^{(0)}(z) + \omega}\int d^4x\sqrt{g}R \\ &= -\alpha_s\frac{1}{2}\frac{1}{(4\pi)^2}\,\mathrm{tr}_s[I]k^2\big(\Phi_1^1(\omega) - \widetilde{\Phi}_1^1(\omega)\big)\int d^4x\sqrt{g}R. \end{aligned} \tag{7.14}$$

Where the definition of the threshold functions (4.48), (4.49) has been used in the second step. As in the previous calculations, $\omega = -2\Lambda_k/k^2$ for the tensor and scalar traces and $\omega = 0$ for the vector trace. The full deformation of the EAA then reads

$$\begin{aligned} \delta\Gamma_k[g,g] = \frac{1}{2}\frac{1}{(4\pi)^2}\int d^4x\sqrt{g}Rk^2\Big[&-(9\alpha_T + \alpha_S)(\Phi_1^1(-2\lambda_k) - \widetilde{\Phi}_1^1(-2\lambda_k)) \\ &+ 8\alpha_V\big(\Phi_1^1(0) - \widetilde{\Phi}_1^1(0)\big)\Big]. \end{aligned} \tag{7.15}$$

Comparing this with the LHS of (2.30), which has the form

$$\delta\Gamma_k[g,g] = 2\kappa^2\int d^4x\sqrt{g}[-R\delta Z_k + 2\delta(Z_k\Lambda_k)], \tag{7.16}$$

we find the deformation of the couplings

$$\delta(Z_k\Lambda_k) = 0, \tag{7.17}$$

$$\delta Z_k = -\frac{1}{4\kappa^2}\frac{1}{(4\pi)^2}k^2\Big[-(9\alpha_T+\alpha_S)(\Phi_1^1(-2\lambda_k)-\widetilde{\Phi}_1^1(-2\lambda_k))+8\alpha_V\big(\Phi_1^1(0)-\widetilde{\Phi}_1^1(0)\big)\Big]. \tag{7.18}$$

The scale evolution of this deformation then follows

$$\begin{aligned}\partial_t\delta Z_k = -\frac{1}{24\kappa^2}\frac{1}{(4\pi)^2}k^2\Big[&-(108\alpha_T+12\alpha_S)(\Phi_1^1(-2\lambda_k)-\widetilde{\Phi}_1^1(-2\lambda_k))+96\alpha_V\big(\Phi_1^1(0)-\widetilde{\Phi}_1^1(0)\big)\\ &-\beta_\lambda\Big((108\alpha_T+12\alpha_S)\big(\Phi_1^2(-2\lambda_k)-\widetilde{\Phi}_1^2(-2\lambda_k)\big)\Big)\Big]\end{aligned} \tag{7.19}$$

Where we have used the identity (A.17) with the chain rule for the derivatives of the Φ functions.
In order to calculate fixed point coordinates, we finish these steps for the total flow equation. Combining (7.19) and the part of (4.51) which contains no α, we find the total flow of the deformed Z_k

$$\begin{aligned}\partial_t Z_k = -\frac{1}{24\kappa^2}\frac{1}{(4\pi)^2}k^2\Big[&(20-108\alpha_T-12\alpha_S)\Phi_1^1(-2\lambda_k)-(10\eta-108\alpha_T-12\alpha_S)\tilde{\Phi}_1^1(-2\lambda_k))\\ &-72\left(\Phi_2^2(-2\lambda_k)-\frac{1}{2}\eta\tilde{\Phi}_2^2(-2\lambda_k)\right)\\ &-(16-96\alpha_V)\Phi_1^1(0)-96\alpha_V\widetilde{\Phi}_1^1(0)-24\Phi_2^2(0)\\ &-\beta_\lambda\Big((108\alpha_T+12\alpha_S)\big(\Phi_1^2(-2\lambda_k)-\widetilde{\Phi}_1^2(-2\lambda_k)\big)\Big)\Big]\end{aligned} \tag{7.20}$$

Once again, we can find η from this equation, like with the contribution from the field transformation, the equation for η is modified:

$$\eta(g_k,\lambda_k) = \frac{g_k B_1^{\delta R_k}(\lambda_k,\alpha_s)}{1-g_k B_2^{\mathrm{FRGE}}(\lambda_k,\alpha_s=0)}, \tag{7.21}$$

where $B_1^{\delta R_k}$ is given by

$$\begin{aligned}B_1^{\delta R_k}(\lambda_k,\alpha_s) = B_1^{\mathrm{FRGE}}(\lambda_k,\alpha_s)+\frac{1}{3}(4\pi)^{-1}\Big[&(108\alpha_T+12\alpha_S)\big(\tilde{\Phi}_1^1(-2\lambda_k)-\Phi_2^2(-2\lambda_k)\big)\\ &-96\alpha_V\big(\widetilde{\Phi}_1^1(0)-\Phi_2^2(0)\big)\\ &+\beta_\lambda\Big(-(108\alpha_T+12\alpha_S)\big(\Phi_1^2(-2\lambda_k)-\widetilde{\Phi}_1^2(-2\lambda_k)\big)\Big)\Big].\end{aligned} \tag{7.22}$$

Here the superscript δR_k indicates the method of deforming the regulator and the flow of this deformed EAA was calculated. Once again, the beta functions have the same structural form (4.53), (4.58). We now have the beta functions for all three methods of computing the flow, and can compare their RG flows and fixed point properties.

7.3 Comparison and Fixed Point analysis

For all three methods the beta functions share the general form (4.53), (4.58), with all α_s-dependence being implicit in the closed form of the anomalous dimension η. Because this general form is preserved, we can immediately conclude that the Gaussian fixed point at $(\lambda_*, g_*) = (0,0)$ is present in all methods for all α_s. The functions B_1, B_2 indicate the difference of the anomalous dimensions of these methods. The functions B_2 are very similar for all three methods because we have neglected the change in the Z_k appearing in front

of the regulator; in the FRGE and FT methods they are the same while the δR_k method uses the $\alpha = 0$ part of these functions. The FT method introduces a new threshold function $\widehat{\Phi}_n^p$ and, compared to the FRGE method, B_1^{FT} has extra terms proportional to the difference $\Phi_1^1 - \widehat{\Phi}_1^1$. One should keep in mind that the FT method should result in an EAA $\widetilde{\Gamma}_k^{(1)}$, i.e. its fixed point should not have an α-dependence.
The δR_k method has extra terms in $B_1^{\delta R_k}$ proportional to the difference $\widetilde{\Phi}_1^1 - \Phi_2^2$ and a term proportional to $\beta_\lambda(\Phi_1^2 - \widetilde{\Phi}_1^2)$. For the purpose of finding fixed points we can ignore the term in η proportional to the beta function of λ_k. When comparing the flows of Z_k (7.19) and (4.51), the contributions from Φ_1^1 match exactly, while the others do not precisely cancel. For the non-Gaussian fixed point, we also see from (4.53) that $\eta = -2$, which makes it so that the $\widetilde{\Phi}_1^1$ contributions of the scalar and tensor parts have exactly the wrong sign for cancellation. It is not directly clear whether the different methods match the expected results when looking at the beta functions, because both the functions B_1 and B_2 are different[19]. A quantitative test can be done with the fixed point by comparing the coordinates and critical exponents. For the fixed point we have the same system of equations (4.59) as in chapter 4, which leads to g_* as a function of λ_*:

$$g_*(\lambda_*) = \frac{2}{2B_2(\lambda_*, \alpha_s) - B_1(\lambda_*, \alpha_s)}. \tag{7.23}$$

We have written this down with the functions $B_1(\lambda_*, \alpha_s), B_2(\lambda_*, \alpha_s)$ without superscript. Naturally, for each method one substitutes the proper B functions. Using this relation we can eliminate the g-dependence in β_λ at the NGFP, so then we have to solve

$$\beta_\lambda(g_*(\lambda_*), \lambda_*) = 0. \tag{7.24}$$

This fixed point condition is numerically solved. As we did in chapter 4 we will set all α_s equal. In figure 6 the fixed point coordinates, as well as the product and fraction of these, are plotted for all three methods as a function of α. The range of α is from -2 to 2, initially ignoring any bounds α should obey. The fixed point exists for all positive α that are used, and the fixed point is destroyed for negative α at around $\alpha = -1.4$ or $\alpha = -1.5$ for the FRGE and FT plots, and around $\alpha = -1.8$ for the δR_k plot. For the δR_k plot the positive valued fixed point is restored when making α more negative, while for the others the fixed point moves to negative values of g_*, λ_*. These negative fixed point values are not plotted so that the scale of the plots is such that we can distinguish the positive fixed point values. The negative fixed point coordinates have larger absolute value than the positive ones, in particular g_* which ranges from -1.6 to -13.5. This transition might occur because the fixed point approaches a singularity in η when decreasing α. Because this behaviour is far outside a range where considering only the terms linear in α (which the Einstein-Hilbert truncation forces us to do) is justifiable, we conclude this behaviour is not significant. In contrast to the example discussed in chapter 5, the qualitative behaviour of the fixed point is stable for α which are not too negative, suggesting that systems with fermions are much more sensitive to a change in coarse graining operator.
As mentioned before, the FT plot has the interpretation of an EAA where the extra terms cancel the α-dependence of the fixed point, since the flow and fixed point is calculated from (7.1). From this one would expect it to be approximately constant with respect to α with fixed point values of around $(\lambda_*, g_*) \simeq (0.3590, 0.2723)$. We see that this is not the case, and for large α values it exhibits the strongest α-dependence of the plots, although one could argue that these large values give unreliable results in this truncation. Furthermore this could be because we neglected the difference in the coupling Z_k appearing in $R_k^{(2)}$ and $R_k^{(1)}$. The overall behaviour of the field transformation method is very similar to that of the FRGE calculation. This can be attributed to the fact that it uses the FRGE result, only adding one extra contribution to it, resulting in similar beta functions. Evidently this contribution is not sufficient to retrieve an α-independent behaviour in this case, and the second extra term appearing in (6.32) needs a fluctuation field to contribute. The plots are numerically quite close to each other for small α, although this can be attributed to them being quite insensitive to α in this range. Finally, since we set all α_s equal, the range of admissible values is

[19] Although the B_2 functions are the same, the FT method uses $B_2(\lambda_k, \alpha_s \neq 0)$ as opposed to $B_2(\lambda_k, \alpha_s = 0)$ and the δR_k method uses $B_2(\lambda_k, \alpha_s = 0)$ as opposed to $B_2(\lambda_k, \alpha_s \neq 0)$

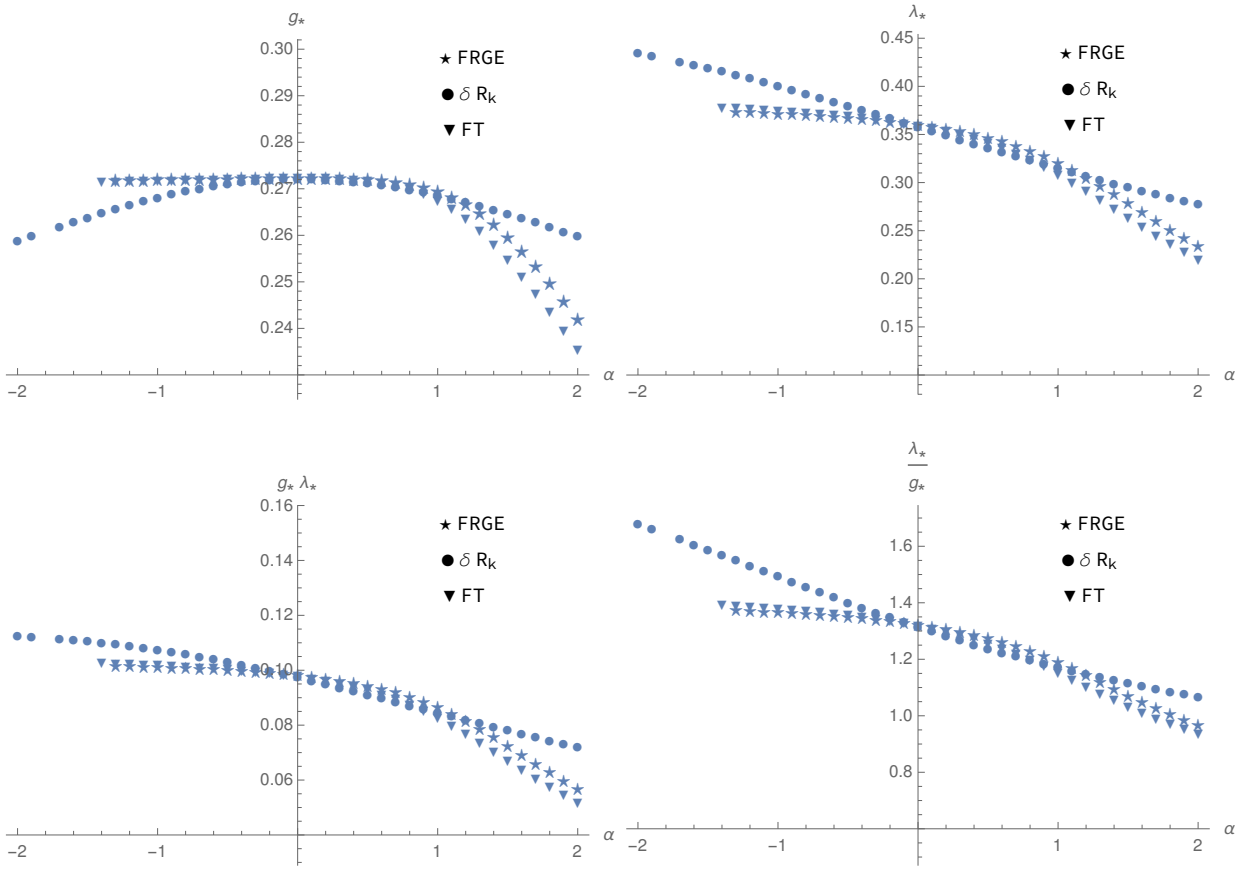

Figure 6: Fixed point coordinates for the three methods, for values of α from -2 to 2. The stars stands for the FRGE calculation, the circles indicate the deformed EAA $\Gamma_k^{(1)} + \delta\Gamma_k$, and the triangles are the result from the field transformation. Negative fixed point coordinates are not plotted in order to keep the scale as is.

empty like in chapter 4.

7.3.1 Critical exponents

To determine the dimension of the UV critical hypersurface and the stability of the non-Gaussian fixed point we want to compute the critical exponents. We go through the steps described in chapter 3.1.1. The critical exponents are numerically calculated for each computation method for values of α from -2 to 2. The result is shown in table 3. The FRGE and FT methods once again yield very similar results: their critical exponents are numerically close and in both cases the fixed point vanishes at similar values for α, after which the fixed point gets negative coordinates (λ_*, g_*) and loses one UV attractive direction. The critical exponents from the δR_k method are numerically more stable than the other two, and their real part curiously reaches a minimum somewhere around $\alpha = -1.0$. This minimum might be thought of as a value of α where the fixed point is the least sensitive to a change in α. Contrary to the other cases, after the fixed point vanishes it is restored at positive (λ_*, g_*) and it still has a two dimensional UV critical hypersurface.

Overall the dependence on α is quite small, in contrast with the gravity-fermion system discussed in Chapter 5, where the fixed point was destroyed for realistic values of α and N_D.

α	θ_n(Field Transformation)	θ_n(FRGE)	θ_n(deformed EAA)
-2.0	(6.63685, -1.68966)	(6.8846, −1.8692)	$1.62328 \pm 8.92047i$
-1.9	(7.03794, -1.29189)	(7.25695, −1.50051)	$1.54534 \pm 8.51858i$
-1.8	(7.63469, -0.906339)	(7.77376, −1.14514)	−
-1.7	(8.71017, -0.520211)	(8.57047, −0.798321)	$1.42839 \pm 7.78994i$
-1.6	(13.5597, -0.0573587)	(10.0989, −0.450919)	$1.38625 \pm 7.45986i$
-1.5	−	(18.0846, −0.059729)	$1.35323 \pm 7.15063i$
-1.4	$0.97263 \pm 5.94801i$	−	$1.32822 \pm 6.86094i$
-1.3	$0.99445 \pm 5.86025i$	$1.00795 \pm 5.63965i$	$1.31024 \pm 6.5896i$
-1.2	$1.01732 \pm 5.76892i$	$1.03082 \pm 5.5632i$	$1.29842 \pm 6.33547i$
-1.1	$1.04135 \pm 5.6738i$	$1.05475 \pm 5.48337i$	$1.29198 \pm 6.09754i$
-1.0	$1.06662 \pm 5.57467i$	$1.07982 \pm 5.39995i$	$1.29023 \pm 5.87482i$
-0.9	$1.09326 \pm 5.47129i$	$1.10614 \pm 5.3127i$	$1.29254 \pm 5.66642i$
-0.8	$1.12138 \pm 5.3634i$	$1.13380 \pm 5.22135i$	$1.29838 \pm 5.47148i$
-0.7	$1.15112 \pm 5.25076i$	$1.16293 \pm 5.12564i$	$1.30723 \pm 5.28917i$
-0.6	$1.18265 \pm 5.13308i$	$1.19365 \pm 5.02528i$	$1.31865 \pm 5.11874i$
-0.5	$1.21616 \pm 5.0101i$	$1.22612 \pm 4.91994i$	$1.33225 \pm 4.95945i$
-0.4	$1.25184 \pm 4.88153i$	$1.26051 \pm 4.8093i$	$1.34765 \pm 4.81059i$
-0.3	$1.28994 \pm 4.74713i$	$1.29701 \pm 4.693i$	$1.36455 \pm 4.67151i$
-0.2	$1.33071 \pm 4.60663i$	$1.33584 \pm 4.57071i$	$1.38266 \pm 4.54156i$
-0.1	$1.37446 \pm 4.45986i$	$1.37725 \pm 4.44205i$	$1.40173 \pm 4.42015i$
0	$1.42153 \pm 4.30669i$	$1.42153 \pm 4.30669i$	$1.42153 \pm 4.30669i$
0.1	$1.47228 \pm 4.1471i$	$1.46901 \pm 4.16432i$	$1.44188 \pm 4.20064i$
0.2	$1.52712 \pm 3.98125i$	$1.52005 \pm 4.01469i$	$1.4626 \pm 4.10148i$
0.3	$1.58644 \pm 3.80951i$	$1.57504 \pm 3.85768i$	$1.48354 \pm 4.00872i$
0.4	$1.65067 \pm 3.63259i$	$1.63444 \pm 3.69335i$	$1.50458 \pm 3.92191i$
0.5	$1.72014 \pm 3.45159i$	$1.69868 \pm 3.522i$	$1.52562 \pm 3.84061i$
0.6	$1.79511 \pm 3.26808i$	$1.7682 \pm 3.34432i$	$1.54655 \pm 3.76442i$
0.7	$1.87562 \pm 3.08417i$	$1.84338 \pm 3.16151i$	$1.56731 \pm 3.69295i$
0.8	$1.96143 \pm 2.90246i$	$1.92444 \pm 2.97535i$	$1.58783 \pm 3.62586i$
0.9	$2.05198 \pm 2.72586i$	$2.01134 \pm 2.7883i$	$1.60806 \pm 3.56282i$
1.0	$2.14628 \pm 2.55731i$	$2.1037 \pm 2.60338i$	$1.62796 \pm 3.50352i$
1.1	$2.24307 \pm 2.39937i$	$2.20071 \pm 2.42397i$	$1.6475 \pm 3.44768i$
1.2	$2.34088 \pm 2.25392i$	$2.30113 \pm 2.25331i$	$1.66665 \pm 3.39505i$
1.3	$2.43827 \pm 2.12189i$	$2.40343 \pm 2.0941i$	$1.6854 \pm 3.34538i$
1.4	$2.53396 \pm 2.00337i$	$2.50599 \pm 1.94803i$	$1.70372 \pm 3.29845i$
1.5	$2.62696 \pm 1.89768i$	$2.60731 \pm 1.81572i$	$1.72162 \pm 3.25406i$
1.6	$2.71659 \pm 1.8037i$	$2.70615 \pm 1.69684i$	$1.73909 \pm 3.21201i$
1.7	$2.80245 \pm 1.72009i$	$2.80173 \pm 1.59033i$	$1.75613 \pm 3.17214i$
1.8	$2.88436 \pm 1.64545i$	$2.89344 \pm 1.4948i$	$1.77274 \pm 3.1343i$
1.9	$2.96233 \pm 1.57847i$	$2.98108 \pm 1.40874i$	$1.78892 \pm 3.09832i$
2.0	$3.03644 \pm 1.51798i$	$3.06459 \pm 1.33065i$	$1.80469 \pm 3.06408i$

Table 3: Critical exponents for the three methods. Entries with a − are values of α for which no fixed point was found. Critical exponents are written down as a 2-tuple when both are real, and are of the form $a \pm bi$ otherwise. Around $\alpha = -1.0$ the δR_k method has an extremum of the real part of the critical exponents.

8 Summary and Conclusion

After reviewing the Renormalization Group in chapters 1 to 4, we took a closer look at the effect of the choice of the coarse graining operator $\Box$ used in $R_k(\Box)$, in particular when it includes an endomorphism term of the form αR. Starting from [2], we saw that this choice can imply different qualitative conclusions regarding asymptotic safety. In order to better understand this, we constructed maps of RG flows obtained from different regulators in chapter 6. Here the central idea was the nonlocal field transformation (6.3). Using this, we have found a relation between the Effective Average Actions and their RG flows. The derivation of these equations provided several interesting insights. First of all, the $k \to 0$ limit of this transformation is in general not well-defined and as a result, this method is best suited for analysis in the ultraviolet. The UV limit of the resulting EAA is well-defined and coincides with the bare action of the EAA without the field transformation. Furthermore, to avoid infinities in the EAA, the path integral needs to be normalized. Also, we can see from (6.21) that the series expansion of the fraction $\frac{R_k^{(2)}}{R_k^{(1)}}$ generates higher momentum terms and with the endomorphism generates higher curvature terms. This insight suggests that higher order momentum and curvature terms generated by the renormalization group by flowing from the UV action S (or from the IR effective action Γ) are less affected by a regulator choice as the order increases. This also hints that enlarging the truncation in chapter 5 with a term $R\bar{\psi}\psi$ might be a good first step in resolving the sign ambiguity found in the fermionic contribution to the gravitational beta function, since this is the first new term generated by the field transformation. Finally, because the map revolves around a field redefinition, it is especially suited to be absorbed into a momentum and curvature dependent wavefunction renormalization constant. In chapter 6.2 we have looked into the commutation of an infinitesimal deformation of the regulator and the scale derivative on the Effective Average Action and concluded these operations commute.

In chapter 7 the exact results were compared to a benchmark calculation done in chapter 4 in an Einstein-Hilbert setting. A comparison was made between an FRGE calculation with a coarse graining operator which included an endomorphism term of the form αR, a calculation (δR_k) where the EAA was deformed according to (2.30); and the relation (6.32) acquired from the field transformation (FT). The chosen truncation is overall quite insensitive to shifts in α, and drastic consequences as seen in chapter 5 only occur for large negative values of α. There are some similarities between the FRGE and δR_k calculation, but the commutation relation established in chapter 6.2 is manifestly broken. Judging from the fixed point properties, we can also see that the FT method has a similar and sometimes stronger α-dependence compared to the other methods, meaning that it is unsuccessful in recovering an α-independent EAA from the α dependent case. There are a number of ways to improve the analysis, which potentially make the proposal more successful:

- Using the modified flow equation proposed in [14]; this flow equation results from normalizing the path integral in the background field formalism and was proposed to make background and fluctuation field equations of motion consistent. By using the Wetterich equation we have not properly regularized the infinities which result from the Jacobian of the field transformation, but instead just ignored them. The modified FRGE gives a well-defined regularization of these infinities.

- A system more sensitive to a change in coarse graining operator might be studied. Presumably this would include fermions like the truncation in chapter 5, in particular enlarging this truncation with an $R\bar{\psi}\psi$ interaction. In general, one can make similar considerations to attempt to diminish regulator effects by including terms expected to be generated by the regulator.

- A fluctuation field computation would likely respond better to the field transformation, since it only works on the fluctuation field. In such a calculation, one would also take the one-point term in (6.32) into account, or even directly compare fixed point coordinates using (6.21).
- One might study structure functions, i.e. couplings that are momentum dependent, since these occur naturally in (6.21). Especially a wavefunction renormalization which includes these dependencies would be suited, as this is closely related to a field transformation.
- Finally, one would expect that in a larger truncation, truncation effects would be smaller. This is still an open question but (6.21) suggests regulator effects get smaller as the order increases. Therefore formal results such as the proposed relation and the commutation relation will be better approximated.

The analysis gave interesting insights on structural properties of the renormalization group and the structure of interactions which might be generated by the presence of the regulator, as well as giving some ideas how to reduce the effect of a regulator choice. Further work could study the formal aspects more, in particular what happens to Ward identities when applying the background dependent field transformation, or apply the formalism to a more involved truncation. One could then follow the template analysis of chapter 7 to compare the methods and see if they converge when enlarging the truncation. Also one can use (6.21) as a guiding principle to determine which terms are largest and should be incorporated first when extending a truncation to help resolve ambiguities caused by a choice of coarse graining operator.

A Heat kernel methods

The RHS of the FRGE is given by a trace over an operator-valued function. In specific scenarios this structure may be cast into a structure where the spectral properties have already been studied in the literature. In the general case, we can use the heat kernel, which is a powerful tool to evaluate operator traces in the context of a derivative expansion.
Typically we will study differential operators of second order

$$\Box \equiv -g^{\mu\nu}\nabla_\mu\nabla_\nu + \mathbf{E}. \tag{A.1}$$

Here $\nabla_\mu \equiv D_\mu + A_\mu$ is a covariant derivative with Levi-Civita connection D_μ and a possible Yang-Mills connection A_μ. $\mathbf{E}$ is an endomorphism on spacetime and internal indices of the field, e.g. $\mathbf{E} = \alpha_s R$. For these cases the heat kernel techniques [30, 31, 32, 33] can be applied. They are based on the heat kernel

$$K(s; x, y; \Box) \equiv \langle x|e^{-s\Box}|y\rangle\,, \tag{A.2}$$

which satisfies the heat equation in d dimensions given an initial condition:

$$(\partial_s + \Box_x)K(s; x, y; \Box) = 0, \qquad K(0; x, y; \Box) = \delta^d(x - y). \tag{A.3}$$

The trace of the operator $e^{-s\Box}$ can then be expressed in terms of the heat kernel at the coincident point $x = y$:

$$\mathrm{Tr}\left[e^{-s\Box}\right] = \int d^dx\sqrt{g}K(s; x, x; \Box). \tag{A.4}$$

The RHS of this equation can then be approximated with various methods. Typical asymptotic expansions include the early-time expansion or late-time expansion. The former is suited for evaluating the gravitational FRGE in a derivative expansion. Thus we will focus on this.

A.1 Early-Time Expansion

The early-time expansion evaluates the trace in (A.4) in terms of an asymptotic series in s

$$\mathrm{Tr}\left[e^{-s\Box}\right] = \frac{1}{(4\pi s)^{d/2}}\int d^dx\sqrt{g}\sum_{n=0}^{\infty}\mathrm{tr}[\mathbf{a}_n s^n]. \tag{A.5}$$

Here the small tr is a trace over internal indices, and the $\mathbf{a}_n$ are constructed from curvature invariants. From this we can see that the early time expansion of K is given by

$$K(s; x, x; \Box) = \frac{1}{(4\pi s)^{d/2}}\sum_{n=0}^{\infty}\mathrm{tr}[\mathbf{a}_n s^n]. \tag{A.6}$$

From dimensional analysis we see that the mass dimension of s is -2 and therefore the mass dimension of $\mathbf{a}_n$ is $2n$. For this reason the early time expansion is well suited for FRGE calculations since terms with $2n$ covariant derivatives appear only in the coefficient $\mathbf{a}_n$. The explicit form of the first few $\mathbf{a}_n$ is given by

[30][20]:

$$\begin{aligned}
\mathbf{a}_0 &= \mathbf{1}, \\
\mathbf{a}_1 &= \frac{1}{6}R\mathbf{1} - \mathbf{E}, \\
\mathbf{a}_2 &= \frac{1}{180}(R^{\mu\nu\rho\sigma}R_{\mu\nu\rho\sigma} - R_{\mu\nu}R^{\mu\nu} + \frac{5}{2}R^2 + 6\nabla^2 R)\mathbf{1} + \frac{1}{12}\Omega_{\mu\nu}\Omega^{\mu\nu} - \frac{1}{6}R\mathbf{E} + \frac{1}{2}\mathbf{E}^2 - \frac{1}{6}\nabla^2\mathbf{E}.
\end{aligned} \tag{A.7}$$

Here $\mathbf{1}$ denotes the unit on internal spin space, and $\Omega_{\mu\nu} = [\nabla_\mu, \nabla_\nu]$. The commutator tensor $\Omega_{\mu\nu}$ different actions depending on if the field is a scalar, vector or symmetric 2-tensor, which can be derived by evaluating them on a field carrying the appropriate internal index structure. For example, for a vector V_α:

$$\Omega_{\mu\nu}V_\alpha = R_{\mu\nu\alpha}{}^\beta V_\beta. \tag{A.8}$$

A.2 Integral Transforms

The FRGE contains find traces over functions $W(\Box)$ of differential operators $\Box$, typically of the form (A.1), which includes both the Levi-Civita and some gauge connection. Equation (A.5) gives the early time expansion of the heat kernel. This can be related to the trace of $W(\Box)$ by means of a Fourier transform. We will use a Fourier transform to relate the trace of W to the heat kernel, just like in chapter 4. The heat kernel can also be used with a Laplace transform. They are easily related by a substitution $s \to is$ in the exponentials and in (A.12)(though not in the integration measure). Note that this does not change (4.45), which holds for both kinds of transforms. We assume $W(z)$ admits a Fourier transform:

$$W(z) = \int_0^\infty ds\ \widetilde{W}(s)e^{isz}. \tag{A.9}$$

here $\widetilde{W}(s)$ is the Fourier transform of $W(\Box)$. Identifying $z = \Box$ and taking the trace this gives

$$\mathrm{Tr}[W(\Box)] = \int_0^\infty ds\ \widetilde{W}(s)\,\mathrm{Tr}\left[e^{is\Box}\right]. \tag{A.10}$$

Evaluting the trace using the early-time heat kernel expansion, this gives

$$\mathrm{Tr}[W(\Box)] = \frac{1}{(4\pi)^{d/2}}\sum_{n=0}^\infty Q_{d/2-n}[W]\int d^dx\sqrt{g}\,\mathrm{tr}[\mathbf{a}_n]. \tag{A.11}$$

The functional Q_n are defined by

$$Q_n[W] \equiv \int_0^\infty ds\ (-is)^{-n}\widetilde{W}(s). \tag{A.12}$$

For positive n these can be related to the original function:

$$Q_n[W] = \frac{1}{\Gamma(n)}\int_0^\infty dz\ z^{n-1}W(z). \tag{A.13}$$

This last identity is proven by substituting (A.9) into (A.13). Then using the integral definition of the gamma function and the identity $\int_0^\infty dz\ z^{n-1}e^{-sz} = s^{-n}\Gamma[n]$, which is found easily by substitution, equation

[20]Because of different conventions there is a difference of a relative minus sign in $\mathbf{E}$ and the Riemann tensor.

(A.12) is found. For negative values of n integration by parts allows us to generalize this relation to

$$Q_n[W] = \frac{(-1)^k}{\Gamma(n+k)} \int_0^\infty dz\; z^{n+k-1} W^{(k)}(z), \tag{A.14}$$

with $W^{(k)}$ being the k-th derivative of W with respect to its argument. The integer k is chosen such that $n + k > 0$.

A.3 Threshold functions

In chapter 4 we have introduced dimensionless threshold functions, which we will repeat here:

$$\Phi_n^p(\omega) \equiv \frac{1}{\Gamma(n)} \int_0^\infty dz\; z^{n-1} \frac{R^{(0)}(z) - zR^{(0)\prime}(z)}{(z + R^{(0)}(z) + \omega)^p}, \tag{A.15}$$

$$\widetilde{\Phi}_n^p(\omega) \equiv \frac{1}{\Gamma(n)} \int_0^\infty dz\; z^{n-1} \frac{R^{(0)}(z)}{(z + R^{(0)}(z) + \omega)^p}. \tag{A.16}$$

Performing a derivative with respect to its argument ω, we easily find

$$\begin{aligned} \frac{\partial}{\partial\omega} \Phi_n^p(\omega) &= -p\Phi_n^{p+1}(\omega), \\ \frac{\partial}{\partial\omega} \widetilde{\Phi}_n^p(\omega) &= -p\Phi_n^{p+1}(\omega). \end{aligned} \tag{A.17}$$

For the exponential cutoff (2.9), no analytic solutions to the integrals of the threshold functions is known. However, for vanishing arguments integrals can be obtained for the generalized exponential cutoffs (2.10) using the polylogarithmic function $\mathrm{Li}_m(s) \equiv \frac{1}{\Gamma[n]} \int_0^\infty dz \frac{s z^{m-1}}{e^z - s}$ and the Riemann zeta function $\zeta(m) = \frac{1}{\Gamma(m)} \int_0^\infty dz \frac{z^{m-1}}{e^m - 1}$. For instance one can find the relation for the exponential cutoff for $p = 1$:

$$\Phi_n^1(0; s) = \frac{n}{s^n} (\zeta(n+1) - \mathrm{Li}_{n+1}(1 - s)) \tag{A.18}$$

Below we list some exact values for the exponential cutoff which can be found with the previous and similar relations.

$$\begin{aligned} \Phi_1^1(0) &= \frac{\pi^2}{6}, & \Phi_2^2(0) &= 1, \\ \widetilde{\Phi}_1^1(0) &= 1, & \widetilde{\Phi}_2^2(0) &= \frac{1}{2}. \end{aligned} \tag{A.19}$$

References

[1] Reuter, M., Saueressig, F. (2018). Quantum Gravity and the Functional Renormalization Group: The Road towards Asymptotic Safety (Cambridge Monographs on Mathematical Physics). Cambridge: Cambridge University Press.

[2] N. Alkofer and F. Saueressig, "Asymptotically safe $f(R)$-gravity coupled to matter I: the polynomial case," Annals Phys. **396** (2018) 173 doi:10.1016/j.aop.2018.07.017 [arXiv:1802.00498 [hep-th]].

[3] 't Hooft, G.; Veltman, M. One-loop divergencies in the theory of gravitation. Annales de l'I.H.P. Physique théorique, Volume 20 (1974) no. 1, pp. 69-94.

[4] M. H. Goroff and A. Sagnotti, "Quantum Gravity At Two Loops," Phys. Lett. **160B** (1985) 81. doi:10.1016/0370-2693(85)91470-4

[5] G. 't Hooft, "Renormalizable Lagrangians for Massive Yang-Mills Fields," Nucl. Phys. B **35** (1971) 167. doi:10.1016/0550-3213(71)90139-8

[6] S. Weinberg, (1979). "Ultraviolet divergences in quantum theories of gravitation". In General Relativity: An Einstein centenary survey: 790-831. Ed. S. W. Hawking and W. Israel. Cambridge University Press.

[7] G. Gubitosi, R. Ooijer, C. Ripken and F. Saueressig, "Consistent early and late time cosmology from the RG flow of gravity," JCAP **1812** (2018) no.12, 004 doi:10.1088/1475-7516/2018/12/004 [arXiv:1806.10147 [hep-th]].

[8] A. Eichhorn, "Status of the asymptotic safety paradigm for quantum gravity and matter," Found. Phys. **48** (2018) no.10, 1407 doi:10.1007/s10701-018-0196-6 [arXiv:1709.03696 [gr-qc]].

[9] C. Wetterich, "Exact evolution equation for the effective potential," Phys. Lett. B **301** (1993) 90 doi:10.1016/0370-2693(93)90726-X [arXiv:1710.05815 [hep-th]].

[10] L. F. Abbott, "The Background Field Method Beyond One Loop," Nucl. Phys. B **185** (1981) 189. doi:10.1016/0550-3213(81)90371-0

[11] M. Reuter, "Nonperturbative evolution equation for quantum gravity," Phys. Rev. D **57** (1998) 971 doi:10.1103/PhysRevD.57.971 [hep-th/9605030].

[12] B. S. DeWitt, "The global approach to quantum field theory. Vol. 1, 2," Int. Ser. Monogr. Phys. **114** (2003) 1.

[13] B. S. DeWitt, "Dynamical theory of groups and fields," Conf. Proc. C **630701** (1964) 585 [Les Houches Lect. Notes **13** (1964) 585].

[14] S. Lippoldt, "Renormalized Functional Renormalization Group," Phys. Lett. B **782** (2018) 275 doi:10.1016/j.physletb.2018.05.037 arXiv:1804.04409[hep-th].

[15] J. Palis. Vector fields generate few diffeomorphisms. Bull AMS 80 (1973), 503-505

[16] M. A. Rubin and C. R. Ordonez, J. Math. Phys.25(1984) 2888; J. Math. Phys.26(1985)65 doi:10.1063/1.526749

[17] A.Lichnerowicz, Spineurs harmonique, C. R. Acad. Sci. Paris Ser. A 257 (1963)

[18] Dirac Operators and Spectral Geometry lecture notes by Joseph C. Varilly, (2006)

[19] R. Percacci, "An Introduction to Covariant Quantum Gravity and Asymptotic Safety," (2017) World Scientific

[20] S. L. Adler, "Einstein Gravity as a Symmetry-Breaking Effect in Quantum Field Theory," Rev. Mod. Phys. **54** (1982) 729 Erratum: [Rev. Mod. Phys. **55** (1983) 837]. doi:10.1103/RevModPhys.54.729

[21] D. M. Capper, J. J. Dulwich and M. Ramon Medrano, "The Background Field Method for Quantum Gravity at Two Loops," Nucl. Phys. B **254** (1985) 737. doi:10.1016/0550-3213(85)90243-3

[22] B. S. DeWitt, "Quantum Theory of Gravity. 2. The Manifestly Covariant Theory," Phys. Rev. **162** (1967) 1195. doi:10.1103/PhysRev.162.1195

[23] M. T. Grisaru, P. van Nieuwenhuizen and C. C. Wu, "Background Field Method Versus Normal Field Theory in Explicit Examples: One Loop Divergences in S Matrix and Green's Functions for Yang-Mills and Gravitational Fields," Phys. Rev. D **12** (1975) 3203. doi:10.1103/PhysRevD.12.3203

[24] N. Nakanishi and I. Ojima, "Covariant operator formalism of gauge theories and quantum gravity," World Sci. Lect. Notes Phys. **27** (1990) 1.

[25] D. F. Litim, "Optimized renormalization group flows," Phys. Rev. D **64** (2001) 105007 doi:10.1103/PhysRevD.64.105007 [hep-th/0103195].

[26] E. Manrique and M. Reuter, "Bimetric Truncations for Quantum Einstein Gravity and Asymptotic Safety," Annals Phys. **325** (2010) 785 doi:10.1016/j.aop.2009.11.009 [arXiv:0907.2617 [gr-qc]].

[27] Lippoldt, Stefan: Fermions in curved spacetimes. PhD thesis. Friedrich Schiller University Jena 2016.

[28] M. Demmel, F. Saueressig and O. Zanusso, "RG flows of Quantum Einstein Gravity in the linear-geometric approximation," Annals Phys. **359** (2015) 141 doi:10.1016/j.aop.2015.04.018 [arXiv:1412.7207 [hep-th]].

[29] H. Gies, "Introduction to the functional RG and applications to gauge theories," Lect. Notes Phys. **852** (2012) 287 doi:10.1007/978-3-642-27320-9_6 [hep-ph/0611146].

[30] D. V. Vassilevich, "Heat kernel expansion: User's manual," Phys. Rept. **388** (2003) 279 doi:10.1016/j.physrep.2003.09.002 [hep-th/0306138].

[31] P.B. Gilkey, (1994), Invariance Theory, the Heat Equation and the Atiyah-Singer Index Theorem, CRC Press, Boca Rotan

[32] I. G. Avramidi, "Heat kernel and quantum gravity," Lect. Notes Phys. Monogr. **64** (2000) 1. doi:10.1007/3-540-46523-5

[33] A. O. Barvinsky and G. A. Vilkovisky, "The Generalized Schwinger-Dewitt Technique in Gauge Theories and Quantum Gravity," Phys. Rept. **119** (1985) 1. doi:10.1016/0370-1573(85)90148-6